



CELECOXIB NIOSOMAL IN-SITU GEL AS A VALUABLE DRUG DELIVERY SYSTEM FOR OCULAR INFLAMMATION

Mohamed S. Ahmed¹, Ikramy A. Khalil^{1*}, Khaled M. A. Hassanein², Gamal A. El-Gendy¹, and Sayed Ismail¹

¹Department of Pharmaceutics, Faculty of Pharmacy, Assiut University, Assiut 71526, Egypt.

²Department of Pathology and Clinical Pathology, Faculty of Veterinary Medicine, Assiut University, Assiut 71526, Egypt

Niosomes are promising nanocarriers for ocular drug administration since they have the potential to enhance the bioavailability and efficacy of different drugs. Meanwhile, topical gels are beneficial for the treatment of ocular inflammation as they improve corneal permeability and increase the contact time with the eye surface. The main purpose of this study was to prepare and evaluate novel niosomal gels for intraocular delivery of celecoxib. Different niosomes were prepared using different surfactants (span 60 and span 40) and cholesterol (30-50 mol %). The optimized formulation made with span 40 and cholesterol (7:3 molar ratio) has a relatively high encapsulation efficiency (~57%) with reasonable particle size for ocular delivery (~348 nm) and showed the highest release of ~65% after 24 hrs compared to other formulations. The optimized niosomal formulation was then used to prepare various formulations of celecoxib in-situ gel and topical hydrogels. The niosomal gels were well tolerated by the eye and showed similar celecoxib corneal permeation. However, the in-situ gel showed a higher anti-inflammatory effect compared to the topical hydrogel and a commercially available diclofenac eye drop. The results shown in this study indicate that celecoxib niosomal in-situ gel is a valuable drug delivery system for ocular inflammation.

Keywords: Celecoxib; niosomes; niosomal in-situ gel; niosomal hydrogel; in-vivo anti-inflammatory effect

INTRODUCTION

Ocular drug delivery systems have limited ocular drug absorption because of a variety of difficulties, including low corneal permeability and the existence of different mechanisms that clear the corneal surface such as lacrimation, tear turnover and tear dilution¹. Traditional ophthalmic solutions have low bioavailability and necessitating frequent instillation of eye drops to produce a therapeutic effect. In addition, there is a possibility of systemic effects from the passage of drugs through the nasolacrimal duct². Enhancing ocular drug absorption requires improved corneal permeability and a longer contact time. The drawbacks of traditional ocular formulations can be efficiently overcome by using the vesicular nanocarrier drug delivery technology. Vesicular systems entrap the drug inside lipid vesicles and allow for prolonged and regulated drug delivery at the corneal surface³. Sustained

administration and increased drug concentration at the site of action result in increased bioavailability. Vesicles additionally protect the drug from enzymatic metabolism at the tear/corneal epithelial surface^{3,4}.

Celecoxib (CXB) is a non-steroidal anti-inflammatory drug that acts by selectively blocking the cyclooxygenase-2 enzyme (COX-2)⁵. COX-2 is a predominant enzyme in the pathophysiology of eye diseases, such as choroidal neovascularization, vascular lesions and diabetic retinopathy⁶. In addition, COX-2 stimulates vascular endothelial growth factor (VEGF), a key factor in the development of proliferative diabetic retinopathy and neovascular age-related macular degeneration. COX-2 also enhances the effects of numerous other soluble inflammatory mediators⁷. Thereby, celecoxib could be used as an anti-VEGF therapy in the treatments of diabetic retinopathy and age-related macular degeneration.

Niosomes have gained popularity as colloidal nanocarriers because of their beneficial properties including controlled drug release over an extended period of time, low toxicity, increased stability and protection of the encapsulated drug from biological environment factors such as enzymatic degradation at the corneal surface^{8,9}.

The most common attempt to increase precorneal residence time involves increasing formulation viscosity (with a moderate impact on the contact time) and developing semi-solid dosage forms, which despite having good retention characteristics, suffer from low patient compliance due to the blurred vision (caused by ointments and gels) and the foreign body sensation they produce^{10,11}. An optimal ophthalmic dosage form can be applied in a liquid form for the patient's point of approval, while ensuring medication retention at the ocular surface and improving bioavailability at the same time¹². In this context, the development of a hybrid drug delivery system which combines the benefits of niosomes as nano-sized vesicular drug carriers and the advantages of accurate dosing and extended ocular residence time offered by the drug delivery platform fulfills the aforementioned objectives.

In-situ gels guarantee sustained drug release, reduce nasolacrimal drainage and reduce systemic absorption by changing from solution to gel under physiological conditions¹³. In addition to improving ocular bioavailability, the *in-situ* gel function as a vehicle for vesicle incorporation may also improve the physicochemical characteristics of celecoxib niosomes in terms of their size distribution, or the homogeneity of the system, maintain celecoxib content during storage and resulting more precisely timed and smoother celecoxib release. Changes in certain physicochemical indicators at the corneal surface such as pH value, ionic composition and temperature may cause the *in-situ* gel to transition from sol to gel¹⁴. On the other hand, niosomal hydrogel formulations for topical application combine the benefits of a modified release and enhanced permeability across the cornea with excellent release properties and a longer residence time on the cornea.

In this study, we prepared niosomes encapsulating celecoxib as a promising system for ocular delivery. The optimized celecoxib niosomal formulation was then incorporated

into *in-situ* gel (*thermo-responsive*) and hydrogels with different gelling agents. The optimized formulations were tested for celecoxib corneal permeability and *in-vivo* anti-inflammatory effect in a rabbit model of induced eye inflammation, compared to a commercialized diclofenac sodium eye drop. The niosomal gels showed similar celecoxib corneal permeation, although the *in-situ* gel showed a higher anti-inflammatory effect compared to the topical hydrogel. The results shown in this study indicate that celecoxib niosomal *in-situ* gel is a valuable drug delivery system for ocular inflammation.

MATERIALS AND METHODS

Celecoxib (CXB) was a kind gift from EL-BORG Pharmaceuticals Inc. (Alexandria, Egypt). Span 60, span 40, cholesterol, poloxamer₄₀₇, hydroxy ethyl cellulose (HEC) and hydroxy propyl methyl cellulose (HPMC) were purchased from Sigma-Aldrich (St. Louis, MO, USA). Dialysis membrane, molecular weight cut-off 12,000–14,000, was purchased from Spectrum Laboratories Inc. (Rancho Dominguez, CA). Chloroform and methanol, HPLC grades, were obtained from Fisher Scientific (Loughborough, Leics, UK). All chemicals and components of buffer solutions were of analytical grade preparations.

Preparation of CXB-loaded niosomes

Niosomes containing CXB were prepared by thin film hydration technique^{1,15}. The composition of different niosomal formulations is shown in **Table 1**. In summary, surfactants, cholesterol in various molar ratios and CXB (10 mg) were precisely weighed and dissolved in a mixture of chloroform: methanol (2:1) in a 250 mL round-bottom flask. A thin dry film of the components developed on the inner wall of the rotating flask as a result of the organic solvent being gradually evaporated at (60 – 70 °C) under reduced pressure using a rotary evaporator at 150 rpm. The dried thin lipid film was then completely hydrated with 10 mL of phosphate buffered saline (PBS, pH 7.4) by rotating the flask in a water bath while operating a rotary evaporator under normal pressure, creating multi-lamellar vesicles and then sonicating for 2 min and storing at 4 °C overnight¹⁶.

Table 1: Composition of different niosomal formulations.

Formulation code	Cholesterol (mol%)	Type of surfactant	Total lipid (μmol)	Surfactant: cholesterol ratio	Drug amount
F1	30	Span 40	300 μmol	7:3	10 mg
F2	40			6:4	
F3	50			5:5	
F4	30	Span 60		7:3	
F5	40			6:4	
F6	50			5:5	
F7	30	Span 40	500 μmol	7:3	
F8	40			6:4	
F9	50			5:5	
F10	30	Span 60		7:3	
F11	40			6:4	
F12	50			5:5	

Determination of encapsulation efficiency

Drug encapsulation efficiency was determined using the dialysis technique for separating the non-entrapped drug from niosomes¹⁷. This procedure involved adding 0.5 mL of CXB-loaded niosomal dispersion into a dialysis bag submerged in 10 mL of distilled water and stirring it magnetically. Every 30 min, free drug was dialyzed; the process was considered finished when there was no drug left in the recipient solution. The total amount of drug contained in non-dialyzed samples was used to calculate the percentage of encapsulation efficiency (E.E%), which was expressed as the proportion of the drug encapsulated into niosomes. By diluting 0.1 mL of dialyzed niosomes to 10 mL of isopropyl alcohol¹⁸ and measuring the absorbance of these solutions at 256 nm using UV-visible spectrophotometer (Shimadzu Seisakusho, Ltd., Kyoto, Japan). This procedure was necessary to break the niosomal membrane by isopropyl alcohol. Each experiment was carried out in triplicate and the results are expressed as mean \pm standard deviation and determined by this equation:

$$(E.E\% = \frac{\text{Amount of entrapped drug}}{\text{Total drug amount}} \times 100).$$

Determination of particle size, polydispersity index and zeta potential

Nano Zetasizer was used to examine the particle size, size distribution patterns and zeta potential of CXB-loaded niosomes (Malvern Instruments, UK). The samples were suitably diluted with PBS before being measured at 25 °C. Hydrodynamic diameter was used to

express niosomal size¹⁹. The measurements were done in triplicate²⁰.

Transmission electron microscopy analysis [TEM]

Transmission electron microscopy was used to describe the morphology of CXB niosomes that had been optimized. Niosomal dispersion was applied for 1 min to a copper grid that had been covered with carbon after being diluted ten times, with the excess being collected with filter paper. A drop of 1% phosphor-tungstic acid was applied as a staining dye to the vesicles²¹. A tip of filter paper was used to blot the excess and it was then allowed to dry. A high-resolution transmission electron microscope (HR-TEM, JEOL JEM 1400, USA) was used to study the morphology of the prepared niosomes and images were taken and processed using imaging viewer software.

Fourier transform infra-red spectroscopy analysis (FT-IR)

CXB, cholesterol, span 40, a blank niosomes and the optimum CXB-loaded niosomes formulation (F1) were all tested using FT-IR spectroscopy (Schimadzu FTIR spectrophotometer). In order to mix the sample with KBr, approximately 1 mg of the pure drug and combination of drug-excipients was introduced and well grounded. Then, using an IR press with an 8-ton pressure, the KBr mixer was pressed to create a palate²². The scanning range was between 4000 and 400 cm^{-1} .

X-ray diffractometry analysis (XRD)

XRD patterns of CXB, cholesterol, span 40, blank niosomes and CXB-loaded niosomes were performed utilizing the XRD-6000 (Shimadzu, Kyoto, Japan) and a copper source to produce K radiation (of 1.5418 Cu). A thin film was created by spreading the material across a micro glass slide. The samples were examined over the temperature range of 4°-59.98° 2 θ at a scanning rate of 0.06° 2 θ /min²³. The X-ray diffraction technique is a common way to assess a compound's crystallinity. The X-ray diffraction patterns of CXB, cholesterol, span 40, blank niosomes and CXB-loaded niosomes were determined.

Differential scanning calorimetry analysis (DSC)

DSC was used to determine the physical state of CXB and the likelihood of drug-excipient interactions within the niosomal vesicles. DSC analysis was performed on the powdered samples of CXB, span 60, cholesterol, dried blank niosomes, lyophilized selected CXB-loaded niosomes and the physical mixture of niosomal components (CXB, Chol and span 60) using computer-interfaced shimadzu calorimeter. About 5 mg of the samples were accurately weighed, sealed in an aluminum pan and heated at a rate of 10 °C/min over a temperature range of 25-350 °C²⁴.

In-vitro drug release and kinetics study of CXB-loaded niosomes

In-vitro release studies of the prepared niosomal formulations were performed using dialysis method²⁵. The acceptor medium contain PBS (pH 7.4) at 37 °C with ethanol (20%) to maintain sink condition²⁶. The cellulose membranes used in dialysis tubing were washed and allowed to soak in distilled water for 24 hrs. Dialysis bags containing a sample of CXB niosomes equivalent to 1.5 mg of CXB was submerged in a 100 mL dissolution medium of PBS (pH 7.4). A thermostatically controlled water bath shaker was used to maintain the dissolving medium at 37 °C at a constant speed of 50 rpm. In order to maintain sink conditions, samples of the acceptor medium were obtained at scheduled times for 24 hrs and replaced with 5 mL of PBS. the absorbance of CXB was measured at 256 nm spectrophotometrically with using PBS

as the blank. Studies of *in-vitro* drug release were performed in triplicate.

Formulation of CXB-loaded niosomal *in-situ* gel (thermo-responsive) and CXB-loaded niosomal hydrogel

Preparation of plain *in-situ* gel (temperature-dependent type)

In-situ thermo-responsive gel formulations containing Poloxamer₄₀₇ (thermos-responsive polymer) were prepared on a weight basis applying the cold method²⁷. The required amount of Poloxamer₄₀₇ (15% w/v, 20% w/v and 25% w/v) was mixed continuously with cold PBS (pH 7.4), equilibrated at 4-6 °C. The resulting dispersions were kept in a refrigerator (4 °C) for around 24 hrs to ensure complete copolymer dissolution.

Preparation of CXB-loaded niosomal *in-situ* gel (temperature-dependent)

CXB-loaded niosomes in equal quantities (1 mg/mL CXB) were gently mixed to form a homogeneous dispersion. To allow for the entire dissolution of the polymer, the required amount of Poloxamer₄₀₇ was distributed in the cooled solution and the mixtures were kept there for approximately 48 hrs for complete dissolution and formation of viscous solution before characterizations²⁸.

Preparation of CXB-loaded niosomal hydrogel

Different CXB gel formulations were prepared (Table 2). CXB-loaded niosomes in equal quantities (1 mg/mL CXB) were gently mixed to form a homogeneous dispersion. HPMC and HEC-based hydrogel were mixed with niosomal dispersion using magnetic stirring to disperse the hydrogel in niosomal dispersion at various concentrations²⁹. the mixtures were stored at 4 ± 2 °C for 24 hrs.

Physicochemical characterization of prepared CXB-loaded niosomal *in-situ* gel and CXB-loaded niosomal hydrogel formulations.

Evaluation of clarity and pH

CXB-loaded niosomal *in-situ* gel and CXB-loaded niosomal gel preparations were inspected for clarity and physical quality before and after the gelation³⁰. A calibrated pH meter was used to measure the pH of preparations before and after gelation.

Table 2: Composition of CXB niosomal *in-situ* gel and hydrogel.

Formulation code	Concentration of polymer% (w/v)	Type of gel	Polymer used
FIG0	15	<i>In-situ</i> gel	Poloxamer407
FIG1	20		
FIG2	25		
F1H1	1.5	Hydrogel	HPMC
F1H2	2		
F1H3	3		
F1H4	1		HEC
F1H5	1.5		
F1H6	2		

Evaluation of gelation capacity of CXB-loaded niosomal *in-situ* gel

The gelation capacity of the samples was tested according to the method described previously^{31,32}. A drop of the tested formulation (40 μ L) was added to 2 mL of freshly made simulated tear fluid (STF) (pH 7.4), which was equilibrated at 35 ± 0.5 °C in a clear container. STF is made up of 100 mL of distilled water, 0.67 g of sodium chloride, 0.2 g of sodium bicarbonate and 0.008 g of calcium chloride dihydrate. The time required for gel formation and gel dissolution was used to calculate the gelation capacity. The experiment was carried out in triplicate.

Evaluation of gelation temperature of CXB-loaded niosomal *in-situ* gel

Using the test tube inversion method, the gelation temperature was assessed in early studies^{33,34}. 5 mL of test formulations were placed in a test tube and submerged in a regulated water bath. Starting at 20 °C and progressing up to 40 °C, the temperature of water bath was raised gradually at a rate of 0.5 °C/min. At each temperature, the sample was given a minute to adjust before the test tube was inverted at a 90° angle. A gelation temperature was established as the temperature at which there was no flow upon inversion.

Evaluation of gelation time of CXB-loaded niosomal *in-situ* gel

Test tube inversion method was also suitable to determine the gelation time of the tested *in-situ* gel formulations^{35,36}. 2 mL of the sample were transferred into a test tube (5 mL) and put in a water bath that was kept at 35 ± 1 °C. The test tube was regularly inverted at a 90°

angle and the amount of time during which no fluidity of the sample was seen for prediction of the gelation time. For every sample, the test was done three times and the average value was determined.

Evaluation of spreadability of CXB-loaded niosomal hydrogels

A spreadability apparatus consisting of two glass slides were used to calculate the spreadability of niosomal hydrogel formulations in triplicate. The upper slides applied force to the sample on the lower slide while the lower slide contained the gel sample. A sample of 0.5 mg of hydrogel was forced between two slides for 1 min. The weight of upper slide is 40 g and the average diameter obtained from each formulation was calculated³⁷. The spreadability was calculated by the following equation:

$$S = m \times L / t$$

where S: spreadability, m: mass of the gel formulation, L: length travel by upper slide and t: time³⁸.

Evaluation of rheology behaviour of CXB niosomal *in-situ* gel and hydrogel

The viscosity of the CXB niosomal *in-situ* gel and hydrogel formulations was measured using a Brookfield digital viscometer (Model DV-II+, Brookfield Engineering Laboratories, INC, Stoughton, MA) outfitted with a helipath stand and T bar spindle. Rheological evaluation for niosomal *in-situ* gel and hydrogel formulations was carried out at different shearing rates (10-100 rpm) and 34 °C (physiological conditions)³⁹, using spindle 96 and the same shear rates, the resulting rheology of *in-situ* gel and hydrogel was determined and

the rheogram was produced⁴⁰. Measurements were performed in triplicates.

***In-vitro* release study of CXB-loaded niosomal *in-situ* gel and hydrogel**

The dialysis method was used to conduct *in-vitro* release studies on niosomal hydrogel formulations and niosomal *in-situ* gels loaded with CXB. The presoaked dialysis tubing cellulose membrane was pipetted with 2 mL of the sample mixture, which is equivalent to 1.5 mg of CXB. The conditions are the same as *in-vitro* release study of CXB-loaded niosomes.

Physical stability study

The optimum CXB-loaded niosomes (**F1**) was kept for 90 days at 4 and 25 °C with measurements of particle size and encapsulation efficiency performed each month⁴¹. Similarly, the optimized CXB-loaded niosomal *in-situ* gel (**F1G1**) and CXB-loaded niosomal hydrogel stored at 4 °C for 90 days with determination of gelation properties, drug content, viscosity and pH values. Meanwhile, CXB-loaded niosomal hydrogel (**F1H1**) stored at 4 and 25 °C for 90 days with measurement of drug content, viscosity, spreadability and pH values.

***Ex-vivo* permeation study**

CXB permeation through the cornea of the rabbit eye was evaluated using the selected formulations of CXB-loaded niosomal *in-situ* gel and hydrogel. The corneas and sclerae of sacrificed rabbits were taken according to the institutional review board of faculty of medicine, Assiut university (Approval no: 17101916). On a membrane (either the cornea or the sclera) attached on one side of an opening glass cylinder, 0.5 mg of the selected CXB-loaded niosomal *in-situ* gel and hydrogel were applied (0.5 cm diameter). The cylinder was submerged in 50 mL of PBS (pH 7.4) used as the release medium^{42,43}. At 37 ± 0.5 °C, the system was shaken for 8 hrs at 50 rpm. As previously noted in the part of *in-vitro* release study, 3 mL aliquots were taken out then replaced with an equivalent volume of the release medium and then subjected to analysis. Experiments were run in three triplicates. Each time point was used to calculate the total amount of CXB that has been permeated through the membrane (either the cornea or the sclera). CXB permeability in non-niosomal

hydrogel and non-niosomal *in-situ* gel was evaluated in a comparable manner.

Evaluation of sterility of the optimized formulations

The sterility testing of eye drops was conducted using the compendial USP <71> method. In order to test for sterility, formulations were incubated for at least 14 days at 30-35 °C in a fluid thioglycolate medium to look for the presence of bacteria⁴⁴ and at 20-25 °C in Sabouraud's agar medium for the prediction of fungal growth in the formulations⁴⁵⁻⁴⁷.

Evaluation of isotonicity of the optimized formulations

A few drops of recently taken blood were put to two slides and one of the slides was then combined with a few drops of an improved formulation. The opposite slide served as the control. Under a microscope, the two slides were compared to look for any differences in the RBCs' structural integrity^{27,44}.

Draize test (eye irritation test)

The selected CXB loaded niosomal *in-situ* gel and hydrogel were assessed using Draize test^{28,48}. Six male albino rabbits weighing between 2 and 3 kg were used in this investigation according to the institutional review board of faculty of medicine, Assiut university (Approval no: 17101916). The rabbits were divided into two groups of three rabbits randomly. CXB-loaded niosomal *in-situ* gel (**F1G1**) was administered to the first group, while CXB-loaded niosomal hydrogel was administered to the second (**F1H1**). Each right eye of the rabbit received 50 µL of the tested niosomal *in-situ* gel within the lower cul-de-sac using a needleless syringe. To prevent the formulation from draining out after instillation, the eyelids of treated eye were carefully kept together for a few seconds. Each untreated contra-lateral eye of the rabbit served as the control (left eye).

Each animal was checked for any signs of irritation, such as swelling, discharge, redness, iris and corneal lesions at 5, 10, 15, 30 min and 1, 2, 4, 8, 12 and 24 hrs post instillation. The experiment was assessed according following criteria, where score 0 corresponds to no redness, inflammation or excessive tearing, 1 corresponds to mild redness with inflammation and slight tearing, 2 corresponds to moderate

redness with moderate inflammation and excessive tearing and 3 corresponds to severe redness and inflammation along with excessive tearing^{28,49,50}.

***In-vivo* assessment of anti-inflammatory effect**

Assessment of treatment of ocular inflammation by optimized CXB-loaded niosomal *in-situ* gel and hydrogel formulations, Epifenac[®] (diclofenac sodium) eye drop, non-niosomal CXB *in-situ* gel and non-niosomal CXB HPMC hydrogel was performed. 21 male albino rabbits weighing between 2 and 3 kg were divided into seven groups each consisting of three rabbits according to the institutional review board of faculty of medicine, Assiut university (Approval no: 17101916). The right eyes of each group were treated with different CXB formulations whereas the left eyes were treated with saline and served as positive control. Group I act as a negative control (normal eye). Group II act as a positive control (inflamed eye by 150 µL carrageenan 0.5% saline solution) and treated with saline. Group III received (50 µL) of the selected CXB-loaded niosomal *in-situ* gel (**F1G1**) (50 µg CXB). Group IV received 50 µL of the selected CXB niosomal hydrogel (**F1H1**). Group V received Epifenac[®] eye drop (diclofenac sodium 1 mg/mL). Group VI received non-niosomal CXB *in-situ* gel. Group VII received non-niosomal CXB HPMC hydrogel.

The instillation of the niosomal *in-situ* gel, niosomal hydrogel and eye drops were done twice daily for 3 successive days after induction. Inflammation was treated for 3 days after 12 hrs from the induction. The alleviation in ocular inflammation is expressed as the average difference between the treated and control groups.

Histopathological studies

Tissue samples from cornea were fixed in 10% neutral buffered formalin. Followed by dehydration by ascending grades of alcohol, clearing by xylene and embedding in paraffin. Sectioning of the tissue with 4-5 microns thick were performed and the sections were stained with hematoxylin and eosin stains (H&E)^{51,52}.

Statistical analysis

Using the GraphPad prism (version 5.0, GraphPad, San Diego, CA programme), one-way analysis of variance (ANOVA) and the

newman-Keuls post-hoc test were used to elucidate the significance between the various groups. The averages of three trials were calculated for each experiment.

RESULTS AND DISCUSSION

Results

***In-vitro* characterization of CXB niosomes**

Twelve formulations of CXB niosomes were prepared using different amounts of lipid, different surfactants and different surfactant:cholesterol ratios as seen in **Table 1**. F1 to F6 were prepared with 300 µmol total lipid while F7 to F12 were prepared with 500 µmol. F1 to F3 and F7 to F9 were prepared with span 40 while F4 to F6 and F10 to F12 were prepared with span 60. In each case, 3 different concentrations of cholesterol were used (30, 40 and 50 mol% of total lipid). The effect of cholesterol concentration, surfactant type and total surfactant/cholesterol ratio on the structure and physicochemical properties of the prepared niosomes is summarised in **Table 3**. FT-IR, XRD and DSC analysis were carried out to further investigate the localization of CXB in niosomes and assess the potential interaction between the drug and niosomal components.

Effect of cholesterol concentration

Cholesterol has been widely used as an additive agent in the preparation of niosomes due to its capacity to increase the membrane's rigidity and enhance the vesicular integrity and stability of niosomes. It has been observed that cholesterol stabilizes the vesicles by modulating the cohesion and mechanical strength of niosomal bilayers. This prevents drug leakage and slows the permeation of solutes contained in the central aqueous cavity of the vesicles.

For span 40 niosomes prepared with 300 µmol total lipid, (F1 to F3) E.E% increased from 57 to 69% by increasing cholesterol amount. Similarly, E.E% increased by increasing cholesterol amount in the case of span 60 niosomes/300 µmol total lipid (F4 to F6, from 63 to ~81%), span 40 niosomes/500 µmol total lipid (F7 to F9 from ~61 to ~74% and span 60 niosomes/500 µmol lipid (F10 to F12, from 69 to ~87%). The highest E.E% was observed in the case of F12 (50 mol% cholesterol, span 60 and 500 µmol lipid) as seen in **Fig. S1**. It has been observed that there is a significant increase in entrapment

efficiency of CXB with increasing cholesterol content from 30 to 50%^{15,53-55}. Additionally, the impact of cholesterol concentration on vesicle size has been studied. The data summarized in **Table 3** revealed that increasing cholesterol amount from 30 to 50 mol% generally results in a significant increase in the particle size in all preparations. The lowest particle size was observed with F4 (30 mol% cholesterol, 310 nm) while the highest particle size was observed with F9 (50 mol% cholesterol, ~765 nm) as seen in **Fig. S2**. This result is similar to the data shown in different literatures^{20,56}. The recognized values for the proper particle size in ophthalmic preparations are generally fewer than 10 μm to prevent eye irritation. Therefore, all formulations tested are generally acceptable for ophthalmic administration. It was observed that the size of the prepared niosomes increased as E.E% increased. Increasing cholesterol amount increases the rigidity of the membranes and more rigid membranes may assemble as larger vesicles. Meanwhile, it was found that CXB was excluded from vesicles prepared with cholesterol amounts >50 mol%, probably because high cholesterol amounts compete with the drug for packing space within the bilayer⁵⁷. It is worth mentioning that increasing cholesterol amount did not significantly affect the charge of the niosomes as seen in **Table 3**.

Effect of type of surfactant

The impact of surfactant type on the E.E% of CXB niosomes and their vesicle size was

investigated (**Table 3**). Using span 60 produced niosomes having E.E% higher than those prepared with span 40 when the total lipid and cholesterol ratio were fixed, for example, F9 (~74%) vs F12 (86%) as shown in **Fig. S1**. In contrast, using span 60 decreased the particle size of niosomes compared to those prepared with span 40, for example, F9 (~765 nm) vs F12 (~706 nm). Niosomes formed by span 60 and cholesterol 50 mol% (F6 and F12) exhibit the highest E.E% (~80 and ~87%, respectively).

Niosomes formed by span 60 and cholesterol 30 mol% (F4 and F10) exhibit relatively low particle size (310 and ~386 nm, respectively) as shown in **Fig. S2**. In controlling drug entrapment within the vesicles, the nonionic surfactant chain length, size of the hydrophilic head group and hydrophilic lipophilic balance (HLB) value are all important factors⁵⁸.

Span 60 shows higher E.E% values compared to span 40 due to its long chain fatty acid (C-18 long saturated stearyl chain), its low HLB value and its high phase transition temperature⁵⁹. Meanwhile, span 60 shows lower particle size compared to span 40 due to its lower HLB value. The hydrophobicity of the non-ionic surfactant is inversely proportional to the diameter of the vesicles. Increased bilayer hydrophilicity as in span 40 results in higher surface free energy, which would result in larger particle sizes^{54,60}.

Table 3: Characterization of different CXB niosomal formulations* (means \pm SD, n = 3).

Formulation code	Cholesterol (mol%)	EE (%)	Particle size (nm)	PDI (nm)	Zeta potential (mV)
F1	30	57.00 \pm 1.00	374.30 \pm 10.3	0.278 \pm 0.042	-26.3 \pm 1.06
F2	40	62.00 \pm 2.54	477.56 \pm 9.80	0.476 \pm 0.039	-24.1 \pm 1.04
F3	50	69.00 \pm 2.20	522.90 \pm 7.91	0.524 \pm 0.015	-25.8 \pm 1.04
F4	30	63.00 \pm 2.10	310.00 \pm 0.21	0.293 \pm 0.021	-27.6 \pm 1.92
F5	40	72.86 \pm 2.86	343.20 \pm 6.06	0.352 \pm 0.100	-30.7 \pm 5.22
F6	50	80.67 \pm 2.15	419.50 \pm 12.0	0.332 \pm 0.037	-34.56 \pm 0.9
F7	30	61.43 \pm 0.81	481.80 \pm 56.0	0.298 \pm 0.204	-22.2 \pm 0.40
F8	40	69.88 \pm 1.87	727.80 \pm 28.9	0.486 \pm 0.135	-25.8 \pm 1.41
F9	50	74.13 \pm 0.47	765.45 \pm 4.17	0.313 \pm 0.047	-28.05 \pm 0.92
F10	30	69.00 \pm 2.00	386.10 \pm 4.82	0.499 \pm 0.325	-28.6 \pm 1.52
F11	40	79.95 \pm 2.05	632.85 \pm 18.5	0.700 \pm 0.066	-32.46 \pm 1.48
F12	50	86.50 \pm 1.95	706.80 \pm 3.10	0.438 \pm 0.090	-35.73 \pm 1.55

Effect of total lipid content

E.E% of CXB in niosomes was increased significantly with increasing the total lipid amount when the surfactant type and cholesterol ratio were fixed, for example, F6 (~81%) vs F12 (~87%) as seen in **Fig. S1**. Similarly, using higher lipid amount (500 μmol) substantially increased the particle size of niosomes compared to those prepared with lower lipid amount (300 μmol), for example, F6 (~420 nm) vs F12 (~707 nm) as seen in **Fig. S2**.

Similar results were obtained in different studies^{53,54}. Increasing the total lipid amount probably increases the number of layers in multilamellar vesicles, which may increase the diameter of the vesicles and encapsulate more drug.

Zeta potential measurement

Zeta potential is essential for the stability of nanoparticles because it determines the type and strength of electrical charges that niosomes develop. Zeta potential ranged from approximately -22 mV to -36 mV. Although the surfactants employed to make the niosomes are nonionic, the examined niosomes are negatively charged, which is sufficient for preventing aggregation and imparting physical stability.

In-vitro release study of CXB-loaded niosomes

The drug release study was conducted for different niosomal formulations (F1 to F6). The amount of CXB released was monitored up to 24 hrs (**Fig. 1**). As can be seen in **Fig. 1B**, increasing the amount of cholesterol from 30 to 50 mol% in the case of span 40 niosomes (from F1 to F3) significantly decreased the amount of CXB released (~65 % to ~32%). Similarly, increasing the amount of cholesterol from 30 to 50% in the case of span 60 niosomes (from F4 to F6) significantly decreased the amount of CXB released (~42% to ~23%). These results are similar to other studies^{61,62}. It is well known that cholesterol prevents the gel to liquid phase

transition of niosomal systems, making niosomes less leaky. This tendency might result from a rise in membrane bilayer rigidity caused by an increase in cholesterol content up to 50 mol%. Meanwhile, span 40 niosomes showed higher drug release compared to span 60 niosomes (F1> F4, ~65 and ~42%) (F2> F5, ~49 and ~36%) and (F3>F6, ~32 and ~23%) (**Fig. 1C**). These results are consistent with previous reports showing that span 60 niosomes produce slower drug release compared to span 40 niosomes⁶³⁻⁶⁵. Niosomes show an alkyl chain length-dependent release. The lower release rates are shown with increasing the alkyl chain length as in the case of span 60 niosomes.

Through exploring the kinetics of drug release from niosomal formulations, it was revealed that CXB release pattern followed the Higuchi diffusion model in all formulations, except for F4, which exhibited a first-order release model. Equation of Higuchi's model is described as following: $Q_t = k_2 t^{1/2}$ Where (Q_t) is the amount of drug released at time t and k_2 is the Higuchi constant^{19,66}.

In order to estimate the diffusion process, the Korsmeyer-Peppas equation $M_t/M = K_{kp} t^n$ was applied. M_t is the amount of drug released at time t , M is the amount of drug released at infinite time and K_{kp} is a Korsmeyer-Peppas constant. It was revealed that the diffusion mechanism experiences non-fickian transport (also known as anomalous diffusion) which involves both diffusion and erosion. The n values of the tested niosomal dispersions were determined to be in the range of 0.64 to 0.88 except F6 ($n = 1.26$) which exhibits non-Fickian transport super case-II as seen in **Table 4**. Based on the release data, **F1** was selected to be the optimized formulation and was further examined in next experiments, it showed the highest release after 24 hrs (~65%).

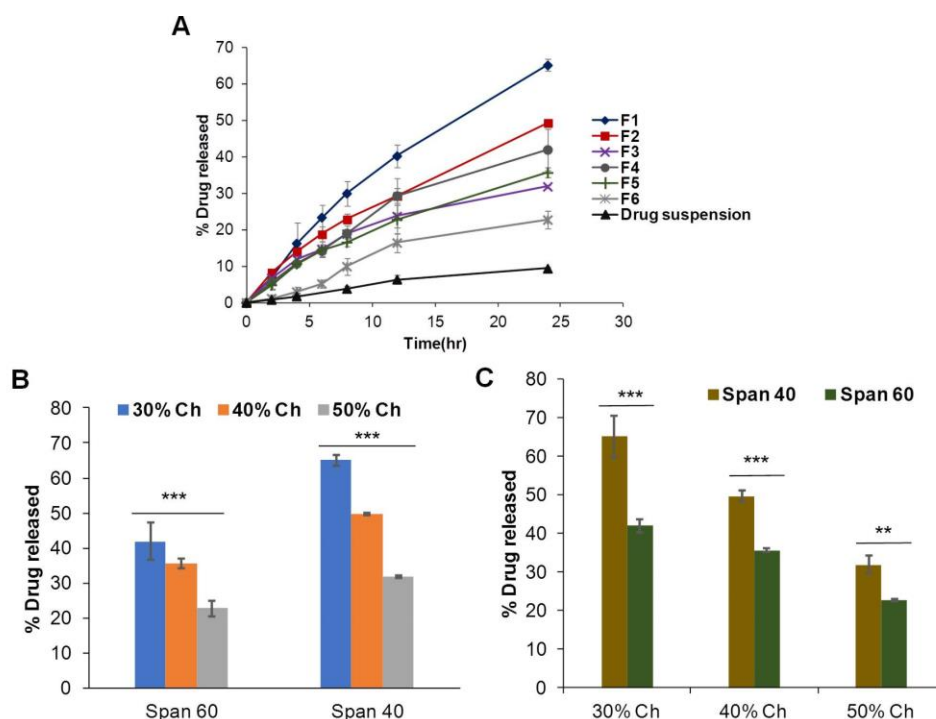


Fig. 1: *In-vitro* release study. A. Release of CXB from different niosomal formulations after 24 hrs. B. Effect of cholesterol content on CXB release. C. Effect of type of surfactant on CXB release. Note: one way ANOVA was used for statistical analysis; * ($P < 0.05$), ** ($P < 0.01$) and *** ($P < 0.001$).

Table 4: Kinetics of CXB release from different niosomal formulations.

Formulation Code	Zero order (r^2)	First order (r^2)	Higuchi model (r^2)	Korsmeyer-Peppas (n)
F 1	0.9764	0.9943	0.9996	0.88
F 2	0.9619	0.9841	0.9883	0.74
F 3	0.9283	0.9504	0.9877	0.64
F 4	0.9723	0.9932	0.9894	0.84
F 5	0.9778	0.9884	0.9979	0.78
F 6	0.9256	0.9386	0.9631	1.26

TEM analysis

Niosomes were examined using TEM to determine their morphology. **Fig. 2** shows the TEM images of the optimized CXB niosomes (**F1**). The TEM image shows that the niosomes were dispersed in the aqueous phase and had a homogeneous spherical shape with a diameter of approximately 100-400 nm. The TEM images confirmed the formation of niosomes.

FT-IR analysis

Fig. 3A shows the IR spectra of the raw materials (span 40, cholesterol and CXB), along with the physical mixture, blank niosomes and CXB-loaded niosomes.

Characteristic peaks of the spectrum of span 40 were seen at 3405, 2918 and 1736.37 cm^{-1} , likely corresponding to the OH, C-H and COO- stretching peaks, respectively. peaks characteristic of cholesterol were seen at 2933 and 3416 cm^{-1} , likely corresponding to OH and C-H stretching. Two forked peaks characteristic of CXB were seen at 3234 and 3340 cm^{-1} , likely corresponding to NH_2 stretching. In the spectrum of the physical mixture, the CXB NH_2 stretching was clearly disappeared and carbonyl stretching (span 40) was clearly visible at 1637.68 cm^{-1} . Furthermore, a broad peak centered around 3417.09 cm^{-1} was seen in the spectrum of the physical mixture, which is most

likely a product of the co-elution of the OH stretching peaks of span 40 and cholesterol. Furthermore, the C=O stretching peak was also visible at 1736.68 cm^{-1} in the spectrum of the physical mixture. In the spectrum of blank niosomes, the OH stretching peak of span 40 was seen to shift to 3440 cm^{-1} . The C-H stretching was seen to shift to 2920.21 cm^{-1} and the COO- stretching peak exhibited a similar shift to 1737.14 cm^{-1} . The shifts observed in the peaks corresponding to the carbonyl groups may be attributed to CXB, span 40 and cholesterol interactions, namely the hydrogen bonding; an interaction characteristic of the formation of niosomes.

In the spectrum of the CXB-loaded niosomes, notable peaks were observed at 3423.87 , 2920 and 1736 cm^{-1} . These peaks likely correspond to the OH, C-H and C=O stretching, respectively. Similar to what was seen in the spectrum of the blank niosomes, significant shifts are observed in the O-H stretching, which are indicative of the interactions mediating the vesicles formation. The disappearance of the NH_2 stretching peak of CXB, which matched with an increase in drug dissolution and the presence of the drug in an amorphous state, refers to a possible incorporation of CXB into the niosomes. This is in agreement with reported findings in the literature⁶⁷⁻⁶⁹.

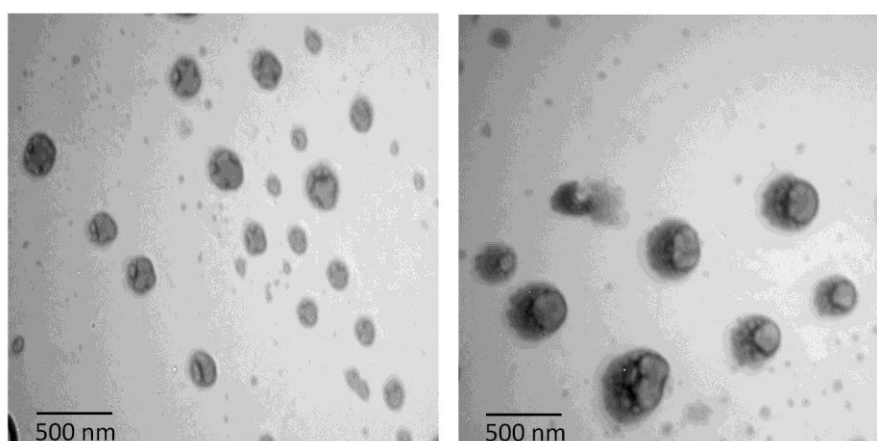


Fig. 2: Transmission electron microscopy of CXB-loaded niosomes (F1).

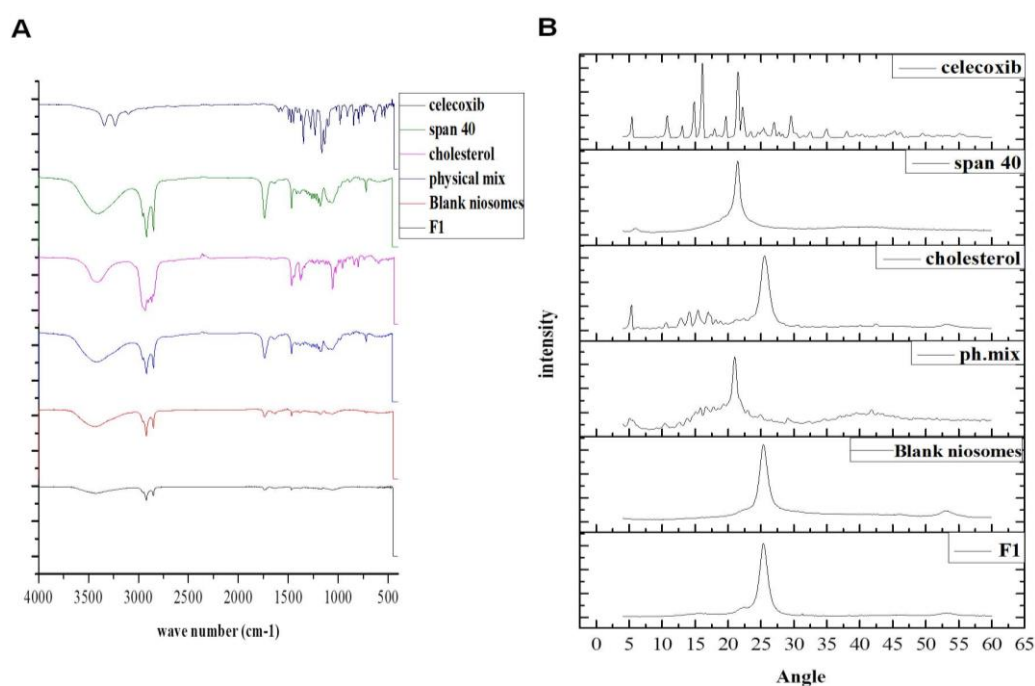


Fig. 3: FT-IR (A) and XRD (B) analysis of CXB-loaded niosomes (F1).

XRD analysis

Pure CXB powder exhibited a numerous sharp peaks at 16.1° , 21.516° , 14.864° and $22.24^\circ 2\theta$. Span 40 showed a single peak at $21.444^\circ 2\theta$ and cholesterol exhibited high intense peak at $25.57^\circ 2\theta$ and low intense peak at $5.342^\circ 2\theta$. XRD diffraction of free CXB and other ingredients confirmed their crystalline nature and the diffraction patterns were in good agreement with the data reported in previous studies⁷⁰⁻⁷². Physical mixture (span 40, cholesterol and CXB) showed a single peak at $21.012^\circ 2\theta$. Blank niosomes spectra presented fused peaks at $25.386^\circ 2\theta$ (almost all characteristic peaks were disappeared). CXB-loaded niosomes showed a single peak ($25.389^\circ 2\theta$) similar to that of blank niosomes which indicates the amorphous structure of the drug and incorporation of CXB within niosomal vesicles and this is complementary to FT-IR data. In this respect, Sadeghi Ghadi and Ebrahimnejad *et al.* reported similar observations⁷³.

DSC analysis

In **Fig. S3**, the DSC thermogram of pure CXB showed a single distinct endothermic peak at 164.5°C . The DSC thermogram of pure cholesterol showed a single distinct endothermic peak at 149.81°C . The DSC thermogram of pure span 60 showed a single distinct endothermic peak at 59.67°C . The DSC thermogram of physical mixture (CXB, cholesterol and span 60) showed a single endothermic peak at 56.76°C . The DSC thermogram of blank niosomes showed a slight shift in the melting temperature of the main constituents (cholesterol and span 60) which might be attributed to the interaction between cholesterol and surfactants in the niosomes. DSC thermogram of CXB-loaded niosomes demonstrated a similar thermal pattern to the blank niosomes with disappearance of the peak of CXB. These results suggest that CXB might be present in an amorphous state inside the niosomes.

Characterization of CXB niosomal *in-situ* gel

Different CXB-loaded niosomal *in-situ* gel formulations were prepared by the cold method in order to establish an optimal concentration necessary to develop a formulation with desired gelation characteristics **Table 5**. The concentrations of poloxamer₄₀₇ which were used are 15% w/v (**F1G0**), 20% w/v (**F1G1**)

and 25% w/v (**F1G2**). To determine the optimum *in-situ* gel composition and to determine whether certain *in-situ* gel bases were suitable for including CXB niosomes, additional rheological experiments and *in-vitro* release studies were conducted on the *in-situ* gel formulations.

Evaluation of clarity and pH

Visual appearance revealed that all prepared plain *in-situ* gels had a colorless and transparent appearance while CXB niosomal *in-situ* gel had a milky appearance. The *in-situ* gel formulations (**F1G1** and **F1G2**) are free flowing liquid at lower temperature ($4 \pm 2^\circ\text{C}$) and when they reached the sol-gel phase transition they turned into gels. The pH values were in the physiologically tolerable range between 6.9 and 7 before gelation and between 6.7 to 6.84 after gelation.

Evaluation of gelation capacity of CXB niosomal *in-situ* gel

Gelation capacities of the *in-situ* gel formulations were visually evaluated according to the following grades: (-) no gelation, (+) gel formation after few minutes, fast dissolution, (++) instantly gel formation, remaining for few hrs, (+++) instantly gel formation, remaining for extended time^{12,74}. The highest gelation capacity was obtained in the case of formulation **F1G2** followed by **F1G1**. In these two formulations, the gelation already occurred at room temperature. The formulation at 15% w/v Poloxamer₄₀₇ concentration (**F1G0**) showed the lowest gelation capacity, which further confirms that the gelation property depends on polymer concentration (**Table 5**).

Evaluation of gelation temperature of CXB niosomal *in-situ* gel

The gelation temperature for **F1G1** and **F1G2** were ~ 27.6 and 24.13°C , respectively, which are well below 30°C . Even when diluted with lacrimal fluid, an optimum *thermo-responsive in-situ* gel formulations converted to gel at a temperature that is between 25 to 34.5°C , ideally below 30°C , to provide precise and reproducible application and a short gelation time^{12,75}. This result may be explained by the differences in the characteristics of the polymer structural blocks, poly (ethylene oxide) (PEO) and poly (propylene oxide) (PPO), that occurred as a result of changes in the polymer concentration or temperature⁷⁶. Poloxamer

copolymers self-associate into micelles in aqueous solution after reaching a specific concentration (critical micellar concentration). Temperature has an influence on this process as well; once the critical micelle temperature is reached, micelles can form at certain concentrations⁷⁷. Poloxamer's PEO and PPO blocks are both hydrated below this point, but as the temperature rises, the PPO block dehydrates causing the development of multi-chain spherical micelles with a dehydrated PPO core and hydrated bloated PEO chains surrounding it^{34,78}. In fact, the appearance of micellar structures may signify the beginning of the gelation process since the various aggregates have a tendency to assemble together and form gel structures^{79,80}. Higher poloxamer concentration contributes to the formation of greater number of micelles, hence achieving $T_{sol-gel}$ phase transition temperatures at lower degrees.

Evaluation of gelation time of CXB niosomal *in-situ* gel

Table 5 illustrates the results of the investigation of the gelation time of CXB niosomal *in-situ* gel formulations. Samples were kept refrigerated before the experiment began. Increasing the concentration of

poloxamer obviously decreased the gelation time from 88.5 sec (F1G1) to 34.3 sec (F1G2). This may be explained by the increased micelles interaction at higher poloxamer concentrations, thus generating the gel structure at a shorter period of time^{81,82}.

Characterization of CXB-loaded niosomal hydrogel

In order to determine the ideal concentration needed to produce a formulation with the desired release pattern and rheological properties, CXB-loaded niosomal hydrogel formulations were made using two types of gelling agents, HPMC (F1H1 to F1H3) and HEC (F1H4 to F1H6) at various concentrations. To confirm their appropriateness for inclusion of CXB niosomes and select the optimum niosomal hydrogel, *in-vitro* release experiments and rheological studies were evaluated.

Evaluation of clarity and pH

Visual evaluation showed that all prepared plain *hydrogels* appeared to be colorless and transparent appearance while CXB niosomal hydrogels showed a milky appearance. The pH values were in the physiologically tolerable range between 6.8 and 7.15 (Table 6).

Table 5: Characterization of different formulations of CXB niosomal *in-situ* gel* (means \pm SD, n = 3).

<i>In-situ</i> gel code	Concentration of poloxamer ₄₀₇	Gelation capacity	Gelation temperature (°C)	Gelation time (sec)	pH before gelling	pH after gelling
F1G0	15% w/v	(-)	-	-	-	-
F1G1	20 % w/v	(+)	27.60 \pm 1.1	88.50 \pm 3.87	6.9 \pm 0.082	6.84 \pm 0.046
F1G2	25% w/v	(++)	24.13 \pm 1.2	34.33 \pm 4.50	7.0 \pm 0.030	6.70 \pm 0.068

(-) no gelation, (+) gel formation after few minutes, fast dissolution, (++) instantly gel formation, remaining for few hours, (+++) instantly gel formation, remaining for extended time.

Table 6: Characterization of CXB niosomal hydrogel* (means \pm SD, n = 3).

Formulation Code	Type of gelling agent	Concentration (% w/v)	pH	Spreadability (g.cm/sec)
F1H1	HPMC	1.5	6.80 \pm 0.014	3.125 \pm 0.190
F1H2		2	6.80 \pm 0.007	2.621 \pm 0.046
F1H3		3	7.00 \pm 0.020	2.132 \pm 0.016
F1H4	HEC	1	6.84 \pm 0.010	3.736 \pm 0.284
F1H5		1.5	7.20 \pm 0.002	2.234 \pm 0.096
F1H6		2	7.15 \pm 0.060	2.078 \pm 0.023

Evaluation of spreadability of CXB-loaded niosomal hydrogel

The CXB niosomal hydrogel formulation (F1H4) has shown the better spreadability compared to other formulations. The result of the spreadability of all the gel formulations are given in descending order as F1H4 > F1H1 > F1H2 > F1H5 > F1H3 > F1H6. Increasing the gelling agent concentration resulted in increase the viscosity which decrease the spreadability value which is in accordance with previous results^{83,84}.

Evaluation of rheology behaviour of CXB niosomal *in-situ* gel and hydrogel

The viscosity values would affect how niosomal *in-situ* gel and hydrogel flow when applied to the eye as well as how the drug is

released. The formulations having larger quantities of the polymers (poloxamer₄₀₇, HPMC and HEC) were more viscous than those containing fewer amounts according to the rheological profile of niosomal *in-situ* gel and hydrogel (Fig. 4). These outcomes might be explained by an increase in the cross-linking of the polymer network⁸⁵. All niosomal *in-situ* gel and hydrogel formulations exhibited pseudo-plastic flow because increasing the angular velocity resulted in reduction in viscosity. The resistance to movement is reduced as molecules orient themselves in the direction of flow. The smooth spreading over the epithelial surface and longer precorneal residence duration are made possible by the pseudo-plastic properties of elaborated *in-situ* gels and hydrogels, which also prevent discomfort during blinking^{86,87}.

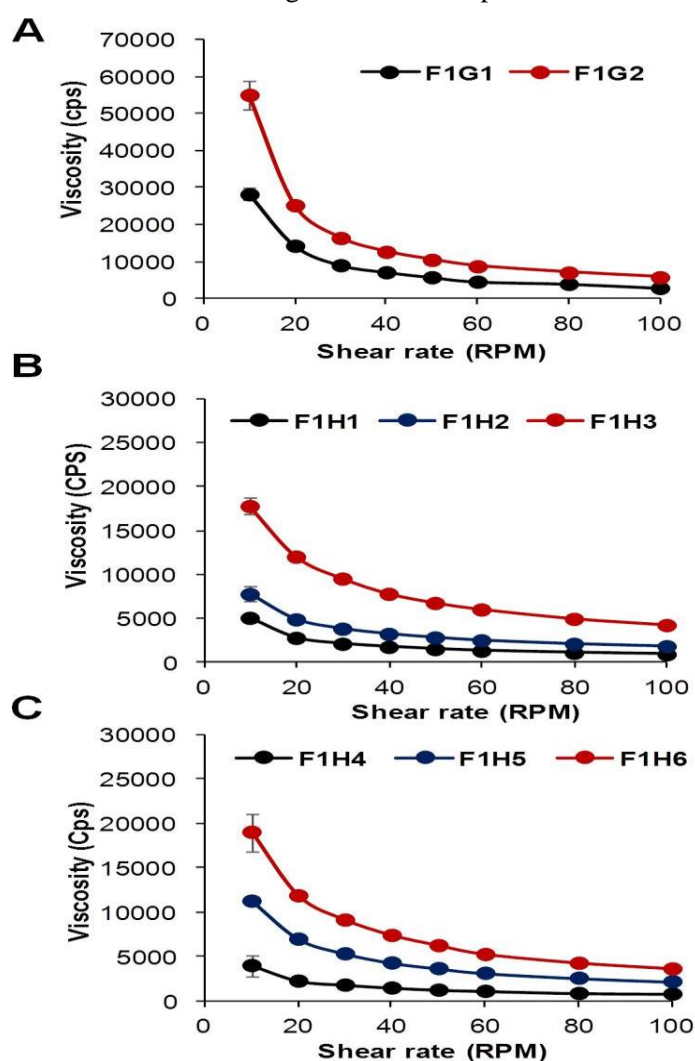


Fig. 4: A. Rheological properties of CXB niosomal *in-situ* gel. B. Rheological properties of CXB niosomal hydrogel (HPMC based). C. Rheological properties of CXB niosomal hydrogel (HEC based). Viscosity values are expressed as centipoises (Cps) and the shear rates are expressed in round per minute (RPM). The data shown are average of 3 independent measurements.

In-vitro release study of CXB niosomal in-situ gel and hydrogel

The pattern of drug release from all prepared niosomal *in-situ* gel and hydrogels with different gelling agents in different concentrations were studied over 24 hrs. For niosomal *in-situ* gel, it was found that increasing the concentration of poloxamer₄₀₇ from 20% (**F1G1**) to 25% (**F1G2**) resulted in a considerable decrease in drug release (*p< 0.05) from (~28% to ~20%, respectively) as shown in **Fig. 5A**. For niosomal based HPMC hydrogel, increasing the concentration of HPMC from 1.5% (**F1H1**) to 3% (**F1H3**) decreased the rate of release significantly (**p< 0.01) from 45.6% to 35.9%, respectively (**Fig. 5B**). However, increasing the concentration of HPMC from 1.5% (**F1H1**) to 2% (**F1H2**) resulted in non-significant decrease in release rate from 45.6% to 41.5%. The comparison of **F1H1** with non-niosomal CXB HPMC based hydrogel showed a significant decrease in rate of drug release in non-niosomal CXB HPMC based hydrogel (*p< 0.05) compared to **F1H1**. For niosomal HEC based hydrogel, increasing concentration of HEC From 1% (**F1H4**) to 1.5% (**F1H5**) resulted in a significant decrease in drug released (*p< 0.05) from 61.24% to 50.46% (**Fig. 5C**). However, increasing concentration of HEC from 1.5% (**F1H5**) to 2%

(**F1H6**) resulted in a non-significant decrease in release (from 50.46% to 47.94%). Increasing concentration of HEC from 1% (**F1H4**) to 2% (**F1H6**) decreased the release significantly from 61.24% to 47.94% (**p< 0.01). Increasing the polymer concentration by 1% is enough for causing a significant difference in release pattern. When comparing F1H4 with non-niosomal CXB HEC-based hydrogel, there is no significant difference in release rate. These outcomes correlated with rheology results because the generated niosomal *in-situ* gel or hydrogel had a higher viscosity with higher polymer concentration since the gels' polymer chains have a high density. The rate of drug release was slowed due to the longer diffusion pathway^{88,89}.

The Higuchi model has the highest r² value of all the release kinetic models for all prepared niosomal *in-situ* gel and hydrogel formulations with non-Fickian transport (n between 0.56 and 0.84) according to the results of the investigation of the mechanism and behavior of drug release as shown in **Table 7**. **F1G1** *in-situ* gel (20% w/v poloxamer₄₀₇) was selected for further experiments because of its higher release pattern. **F1H1** hydrogel (HPMC based) was selected for further experiments because HPMC is more tolerable by the eye than HEC.

Table 7: Kinetics of CXB release from different *in-situ* gel and hydrogel formulations.

Formulation Code	Zero order (r ²)	First order (r ²)	Higuchi model (r ²)	Korsmeyer-Peppas (n)
F1G1	0.9618	0.9766	0.9956	0.75
F1G2	0.8184	0.8378	0.9273	0.84
F1H1	0.8539	0.9111	0.9406	0.56
F1H2	0.8654	0.9108	0.9566	0.76
F1H3	0.8890	0.9277	0.9691	0.73
F1H4	0.9761	0.9990	0.9993	0.69
F1H5	0.9593	0.9877	0.9978	0.61
F1H6	0.9752	0.9900	0.9908	0.64

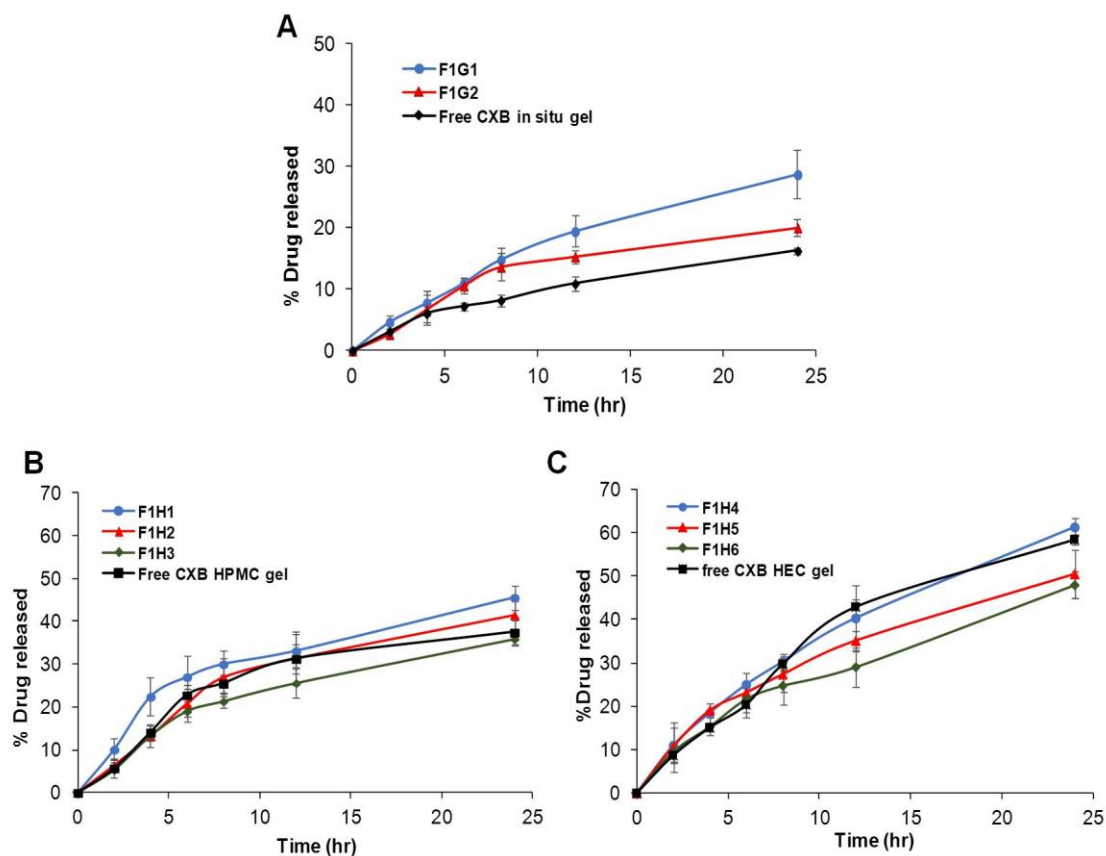


Fig. 5: A. *In-vitro* release study of CXB niosomal *in-situ* gel. B. *In-vitro* release study of CXB niosomal hydrogel (HPMC based). C. *In-vitro* release study of CXB niosomal hydrogel (HEC based).

Physical stability study

The optimal niosomal formulation (**F1**) was stable for up to 2 months when stored at 4 °C regarding particle size, PDI and E.E%. When stored at room temperature, drug leakage was observed every month (E.E% was decreased from 57 to ~38%) and the particle size was increased (from 348 to 429 nm) through 3 months, increasing the mean diameter of vesicles when stored at room temperature may be due to the fusion or aggregation of the vesicles as shown in **Table S1**.

F1G1 and **F1H1** are selected for stability study of CXB niosomal *in-situ* gel and hydrogel. For CXB niosomal *in-situ* gel (**F1G1**), there is no significant difference in pH at first 2 months but increased significantly after 3 months (**P value < 0.001). There is no significant difference in the gelation time and temperature, and viscosity at 4-8 °C for 3 months as seen in **Table S2**. For CXB niosomal

hydrogel (**F1H1**), refrigerated samples (stored at 4-8 °C) withhold their characters regarding pH till 2 months and viscosity till 3 months as the viscosity reduced from 5100 ± 278 Cps to 4937 ± 618 Cps during storage of CXB niosomal hydrogel at 4-8 °C as shown in **Table S3**. During storage at room temperature the viscosity reduced significantly from 5100 ± 278 Cps to 3375 ± 530 (**P value < 0.01) as shown in **Table (S3)**. The drug content during storage at 4-8 °C reduced significantly from 96.56 ± 4.4 to 84.16 ± 3.2 (*P value < 0.05) after 3 months, similarly at 25 ± 2 °C (ambient temperature), the drug content reduced significantly to $75.8\% \pm 1.2$ (**P value < 0.001) as seen in **Table S3**. Based on these results, the optimized formulation should be stored in the refrigerator to maintain better stability.

Ex-vivo permeation study

The study of the corneal permeability of selected formulations (**F1G1** and **F1H1**) was conducted using non-niosomal drug *in-situ* gel and hydrogel preparations as controls. The cumulative amount of CXB that passed through the rabbit cornea using different formulations is presented as a function of time (**Fig. 6A** and **6B**). The influence of niosomes on corneal permeation of CXB was evaluated through studying *ex-vivo* permeation for **F1G1** (20% poloxamer₄₀₇) and **F1H1** (1.5% HPMC) against non-niosomal drug *in-situ* gel and HPMC based hydrogel, respectively. It was found that a significant (***p*<0.01) increase in the amount of CXB permeated from **F1G1** (87.526 mcg.cm⁻²) compared to that permeated from non-niosomal drug *in-situ* gel preparation (53.407 mcg.cm⁻²) after 8 hrs. For selected **F1H1** there is a significant increase (***p*<0.01) in the amount of CXB permeated (96.983 mcg.cm⁻²) compared to that permeated from

non-niosomal HPMC based gel (61.551 mcg.cm⁻²). There is no significant difference between **F1G1** and **F1H1** for the amount of CXB permeated. The proper amount of cholesterol was present in the formulation, which improved medication permeation by giving the niosomal bilayer more strength while also improving the permeability and stability of the resulting bilayer. This is due to the ability of cholesterol to lower the temperature peak during vesicle phase transitions while simultaneously raising the chain order of the liquid state bilayer^{60,90}. CXB permeation into rabbit cornea was measured (**Table 8**) and the amount (*Q*) was plotted against time. The slope of the linear portion of the figure was used to compute the transdermal drug flux (*J_{ss}*). The apparent permeability coefficient (*P_{app}*) was determined through [*J_{ss}* / *C_o*] equation where *C_o* is the initial drug concentration⁹¹. The two formulations selected for *in-vivo* evaluation.

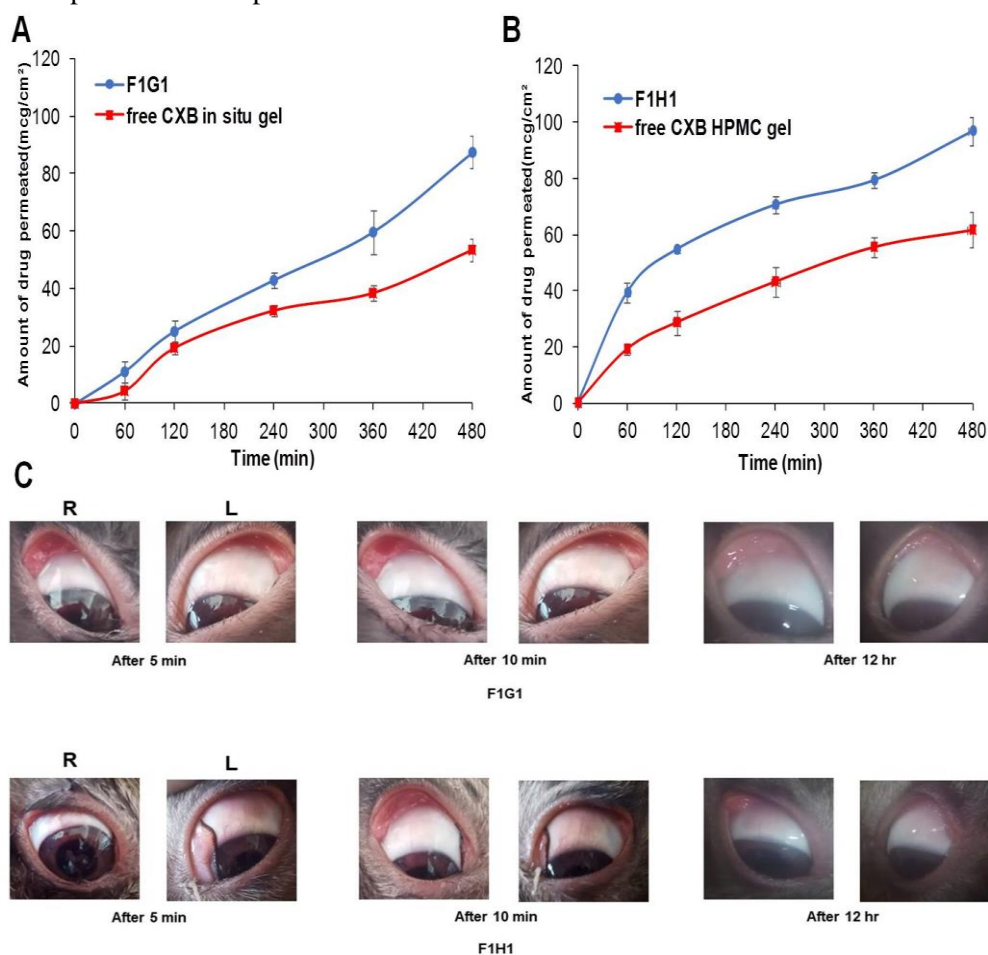


Fig. 6: A. *Ex-vivo* permeation study of CXB niosomal *in-situ* gel (F1G1). B. *Ex-vivo* permeation study of CXB niosomal hydrogel (F1H1). C. Draize test to evaluate the eye irritation after administration of optimized CXB niosomal formulations (R = right eye (treated), L = left eye (control)).

Table 8: *Ex-vivo* permeability parameters* (means \pm SD, n = 3).

Parameter	Q	J _{ss}	P _{app}
Formulation code	(mcg.cm ⁻²)	(mcg.cm ⁻² .h ⁻¹)	(cm/hr)
F1G1	87.526 \pm 5.789	10.507 \pm 0.2962	0.0105 \pm 0.00030
Free <i>in-situ</i> gel (non-niosomal)	53.407 \pm 5.367	6.5782 \pm 0.4096	0.0066 \pm 0.00035
F1H1	96.983 \pm 7.107	10.310 \pm 0.5765	0.0103 \pm 0.00056
Free HPMC gel (non-niosomal)	61.551 \pm 8.880	7.2934 \pm 0.7365	0.0073 \pm 0.00070

Evaluation of sterility of the optimized formulations

The sterility testing was performed on the optimized niosomal *in-situ* gel and niosomal hydrogel for detecting bacterial and fungal growth. The preparations were incubated in thioglycolate broth media (at 34 °C) and Sabouraud's medium (at 20-25 °C) and any sign of bacterial or fungal growth were observed after 14 days of incubation. All tubes showed no signs of precipitate, indicating no growth of bacteria and fungi (**Fig. S4** and **S5**). Methyl paraben was used as a preservative and added to all CXB niosomal *in-situ* gel and niosomal hydrogel formulations.

Evaluation of isotonicity of the optimized formulations

Isotonicity was evaluated by mixing the tested samples with few drops of blood and searching for possible changes in the form or shape of the red blood cells under a microscope. The tested formulations did not show any change in the integrity of the red blood cells as illustrated in **Fig. S6**, confirming the isotonicity of the two tested formulations compared to the control isotonic, hypertonic and hypotonic solutions. The isotonicity is an indicator of eye irritation upon administration.

Draize test (eye irritation test)

After 5 and 10 min of the application of the two selected formulations (**F1G1** and **F1H1**), the modified Draize test showed a slight redness of the conjunctiva but no chemosis (**Fig. 6C**). The irritation score not exceeding 4 is generally acceptable⁴⁸. In this study, the irritation score didn't exceed 2 in any of the six rabbits during the time tested. The two formulations showed no evidence of ocular irritation, such as redness, tearing or swelling indicating that they are not irritating to the eye.

In-vivo anti-inflammatory assessment

Fig. 7 shows the anti-inflammatory effects of different CXB niosomal *in-situ* gel (**F1G1**) and CXB niosomal hydrogel (**F1H1**) after induction of ocular inflammation by carrageenan (0.5%) in saline solution^{92,93}. Marketed NSAIDs (diclofenac sodium) (Epifenac[®] eye drop), non-niosomal CXB *in-situ* gel and non-niosomal CXB hydrogel were used as different controls. The inflammation scores were recorded based on Draize eye test⁴⁹. The inflammation score for CXB loaded niosomal *in-situ* gel (**F1G1**) demonstrated significantly faster recovery than Epifenac[®] eye drop, CXB niosomal hydrogel (**F1H1**), non-niosomal CXB *in-situ* gel, non-niosomal CXB HPMC gel and saline (positive control). The *in-situ* gel (**F1G1**) reduced the induced inflammatory signs significantly by ~ 66% (score 1) on the first day and complete recovery (score 0) was achieved on day 2. Meanwhile, Epifenac[®] eye drop slightly reduced the inflammatory signs (score 2.5) on the first day and complete recovery was achieved on day 3. In the case of CXB niosomal hydrogel (**F1H1**), the inflammatory signs weren't improved on the first day (score 3) and complete recovery was not achieved on day 3 (score 1). Different *in-situ* gel and hydrogel containing non-niosomal CXB didn't show complete recovery up to 3 days (**Fig. 7**). The slower recovery rate in the case of niosomal hydrogel compared to the *in-situ* gel may be attributed to the difficulty of application and lower mucoadhesion (lower viscosity) of niosomal hydrogel⁹⁴. The anti-inflammatory effect of non-niosomal CXB *in-situ* gel is probably due to the presence of poloxamer₄₀₇, which may aid the solubilization of hydrophobic drugs more than the water-soluble polymer HPMC used in hydrogel.

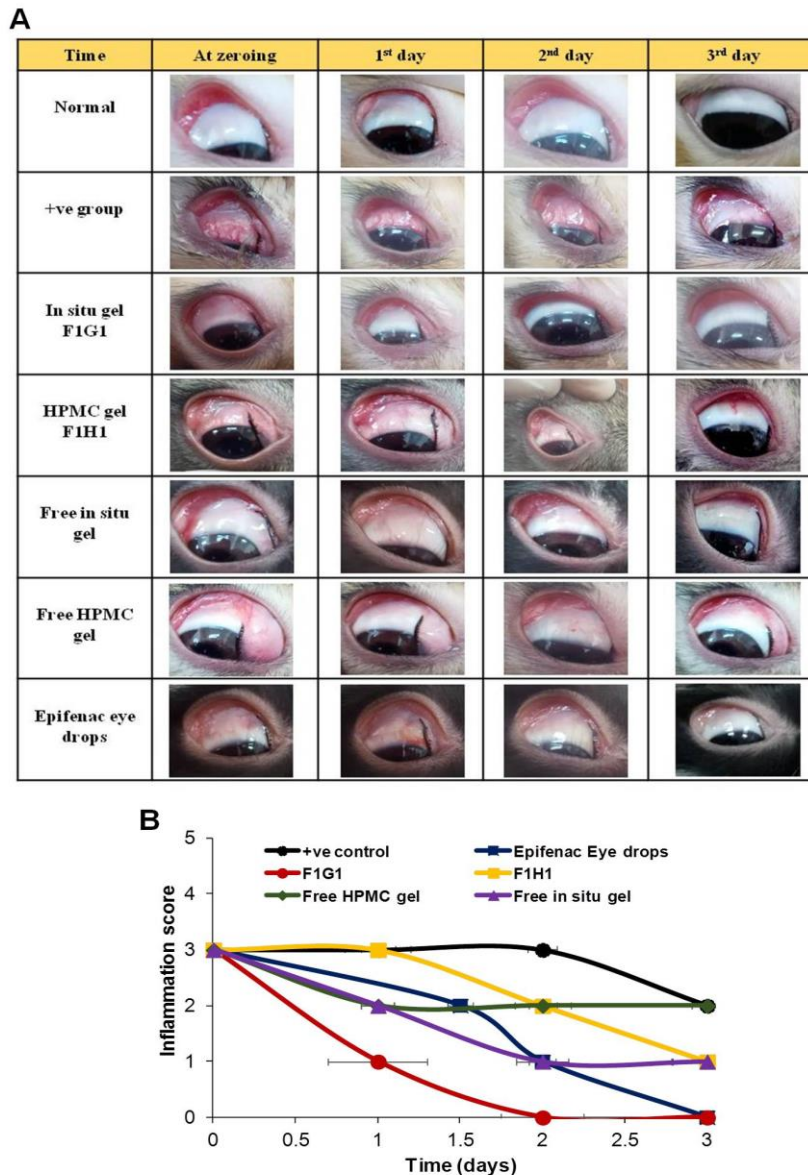


Fig. 7: A. *In-vivo* assessment of the anti-inflammatory effect of different CXB formulations. B. Numerical scoring of inflammation for 3 days for each treated group.

Histopathological study

The eyes of different rabbits were histologically examined by the end of day 3 (**Fig. 8**). Examination of the central part of cornea which was stained by H&E in normal rabbits (**Fig. 8 A, B**) revealed normal corneal epithelium, stroma and descemet's membrane. Histopathological examination of rabbits with induced eye inflammation treated with saline (positive control) showed necrosis of the epithelium with multiple areas of ulceration, necrosed stroma and infiltration with inflammatory cells in the form of neutrophils and lymphocytes (**Fig. 8C, D**). CXB niosomal *in-situ* gel (**F1G1**) treated group showed normal epithelium, normal stroma and normal

descemet's membrane on day 3 (**Fig. 8E, F**). CXB niosomal hydrogel (**F1H1**) treated group showed ulceration in the epithelial lining (**Fig. 8G**). Non-niosomal CXB *in-situ* gel treated group showed necrosis and ulceration of the lining epithelium, necrotic stroma and destruction of descemet's membrane (**Fig. 8H**). Non-niosomal CXB hydrogel treated group revealed necrosis and ulceration of the lining epithelium and infiltration of inflammatory cells in the stroma (**Fig. 8I, J**). Epifenac® treated group revealed normal epithelium, edema in the stroma and destruction of descemet's membrane (**Fig. 8K, L**).

These results support the *in-vivo* anti-inflammatory study shown in **Fig. 7** and

confirm the superior effects of the niosomal *in-situ* gel compared to other formulations.

In this study, CXB-loaded niosomes were prepared for the first time for ocular delivery for treatment of eye inflammation. While CXB-loaded niosomes were previously prepared as a transdermal gel for treatment of skin inflammation, there are no reports about the preparation of CXB-loaded niosomes for ocular delivery. The ophthalmic dosage form has additional requirements compared to the topical one such as sterility, isotonicity and buffer adjustment. In this study, CXB niosomes are formulated into a *thermo-responsive in-situ* gel (using poloxamer 407) and topical hydrogels (using HPMC and HEC) for comparison. Such a comparison of different gel formulations is also performed for the first time. This study showed that although the corneal permeation of celcoxib was similar in selected formulations (*in-situ* gel vs. HPMC-based hydrogel), the anti-inflammatory effect was significantly higher in the case of *in-situ* gel. In contrast, a higher drug release was observed in the case of HPMC-hydrogel. These results indicate that the *thermo-responsive in-situ* gel is the only type

that achieved the aims of sustaining drug release and permeability and prolonging the contact time due to its mucoadhesive properties resulting in improved bioavailability and decreased frequency of dosing. In this study, poloxamer₄₀₇ *in-situ* gel (temperature-dependent) with *in-situ* gel prepared using carbopol 934 (pH-sensitive) or gellan gum (ion-activated) (data not shown). Carbopol-based *in-situ* gel was not applicable in this study because the pH of the niosomal dispersion (7.4) is above the PK_a of carbopol (5.5). Similarly, gellan gum-based *in-situ* gel was not applicable due to the presence of salts in niosomal dispersion buffer system. Both carbopol-based and gellan gum-based *in-situ* gels were converted into gel at once after preparation before application to the eye. Therefore, the poloxamer-based *in-situ* gel was selected since it was the only formulation that remained in the liquid state before application and rapidly converted to gel after application.

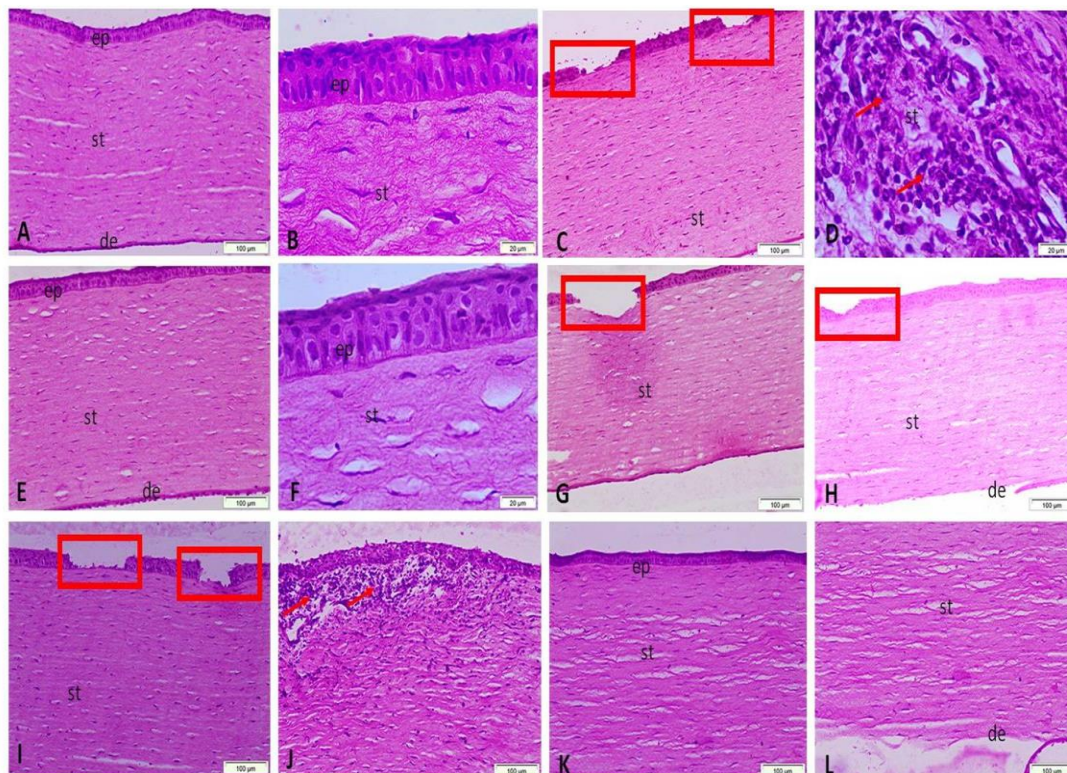


Fig. 8: Histopathological study of rabbits treated with or without different CXB formulations.

Normal eye (A&B), induced inflamed eye (C&D), FIG1 *in-situ* gel (E&F), F1H1 hydrogel (G) non-niosomal *in-situ* gel (H), non-niosomal hydrogel (I&J) and Epifenac[®] eye drop (K&L).

Conclusion

CXB niosomes proved to be a promising tool for delivering CXB to the eye. CXB niosomal *in-situ* gel showed the highest anti-inflammatory effect compared to CXB niosomal hydrogel and commercially available non-steroidal anti-inflammatory eye drop. Incorporation of CXB into niosomes improved drug solubility and provided sustained drug release. The use of *in-situ* gel prolonged the contact time and improved the drug permeation and absorption due to the solubilization effect of poloxamer₄₀₇. The *in-situ* gel also offers the advantages of ease of application and facilitated distribution into the eye and improved mucoadhesion after transition into gel subsequent to administration. CXB niosomal *in-situ* gel proved to be a valuable drug delivery system for ocular inflammation.

REFERENCES

1. G. Abdelbary and N. El-Gendy, "Niosome-encapsulated gentamicin for ophthalmic controlled delivery", *AAPS PharmSciTech*, 9(3), 740-747 (2008).
2. M.K. Arıcı, D.S. Arıcı, A. Topalkara, and C. Güler, "Adverse effects of topical antiglaucoma drugs on the ocular surface", *Clin Experiment Ophthalmol*, 28(2), 113-117 (2000).
3. Y. Pathak, V. Sutariya, and A.A. Hirani, "Nano-biomaterials for ophthalmic drug delivery", *Springer* (2016).
4. I. P. Kaur, A. Garg, A.K. Singla, and D. Aggarwal, "Vesicular systems in ocular drug delivery: An overview", *Int J Pharm*, 269(1), 1-14 (2004).
5. S. J. Kim, A.J. Flach, and L.M. Jampol, "Nonsteroidal anti-inflammatory drugs in ophthalmology", *Surv Ophthalmol*, 55(2), 108-133 (2010).
6. Y. Du, V.P. Sarthy, and T.S. Kern, "Interaction between no and cox pathways in retinal cells exposed to elevated glucose and retina of diabetic rats", *Am J Physiol Regul Integr Comp Physiol*, 287(4), R735-R741 (2004).
7. S.C. Maloney, B.F. Fernandes, E. Castiglione, E. Anteckka, C. Martins, J.C. Marshall, S. Di Cesare, P. Logan, and M.N. Burnier Jr, "Expression of cyclooxygenase-2 in choroidal neovascular membranes from age-related macular degeneration patients", *Retina*, 29(2), 176-180 (2009).
8. R.K. Sahoo, N. Biswas, A. Guha, N. Sahoo, and K. Kuotsu, "Nonionic surfactant vesicles in ocular delivery: Innovative approaches and perspectives", *Biomed Res Int*, 2014, ID 263604 (2014).
9. P.L. Yeo, C.L. Lim, S.M. Chye, A.P.K. Ling, and R.Y. Koh, "Niosomes: A review of their structure, properties, methods of preparation, and medical applications", *Asian Biomed*, 11(4), 301-314 (2017).
10. K. Edsman, J. Carlfors, and R. Petersson, "Rheological evaluation of poloxamer as an in situ gel for ophthalmic use", *Eur J Pharm Sci*, 6(2), 105-112 (1998).
11. Z.M. Fathalla, A. Vangala, M. Longman, K.A. Khaled, A.K. Hussein, O.H. El-Garhy, and R.G. Alany, "Poloxamer-based thermoresponsive ketorolac tromethamine in situ gel preparations: Design, characterisation, toxicity and transcorneal permeation studies", *Eur J Pharm Biopharm*, 114, 119-134 (2017).
12. H. Qi, W. Chen, C. Huang, L. Li, C. Chen, W. Li, and C. Wu, "Development of a poloxamer analogs/carbopol-based in situ gelling and mucoadhesive ophthalmic delivery system for puerarin", *Int J Pharm*, 337(1-2), 178-187 (2007).
13. Y. Wu, Y. Liu, X. Li, D. Kebebe, B. Zhang, J. Ren, J. Lu, J. Li, S. Du, and Z. Liu, "Research progress of in-situ gelling ophthalmic drug delivery system", *Asian J Pharm Sci*, 14(1), 1-15 (2019).
14. A.A. Al-Kinani, G. Zidan, N. Elsaid, A. Seyfoddin, A.W. Alani, and R.G. Alany, "Ophthalmic gels: Past, present and future", *Adv Drug Deliv Rev*, 126, 113-126 (2018).
15. S. Moghassemi and A. Hadjizadeh, "Nano-niosomes as nanoscale drug delivery systems: An illustrated review", *J Control Release*, 185, 22-36 (2014).
16. M. Gharbavi, J. Amani, H. Kheiri-Manjili, H. Danafar, and A. Sharafi, "Niosome: A promising nanocarrier for natural drug delivery through blood-brain barrier", *Adv Pharmacol Sci*, 2018, 6847971 (2018).
17. R. Muzzalupo, L. Tavano, F. Lai, and N. Picci, "Niosomes containing hydroxyl

- additives as percutaneous penetration enhancers: Effect on the transdermal delivery of sulfadiazine sodium salt", *Colloids Surf B Biointerfaces*, 123, 207-212 (2014).
18. A. Zaid Alkilani, H. Abu-Zour, A. Alshishani, R. Abu-Huwajj, H.A. Basheer, and H. Abo-Zour, "Formulation and evaluation of niosomal alendronate sodium encapsulated in polymeric microneedles: In vitro studies, stability study and cytotoxicity study", *Nanomater*, 12(20), 3570 (2022).
 19. R. Gouda, H. Baishya, and Z. Qing, "Application of mathematical models in drug release kinetics of carbidopa and levodopa er tablets", *J Dev Drugs*, 6(2), 1-8 (2017).
 20. V. Gugleva, S. Titeva, S. Rangelov, and D. Momekova, "Design and in vitro evaluation of doxycycline hyclate niosomes as a potential ocular delivery system", *Int J Pharm*, 567, 118431 (2019).
 21. A. Mirzaie, N. Peirovi, I. Akbarzadeh, M. Moghtaderi, F. Heidari, F.E. Yeganeh, H. Noorbazargan, S. Mirzazadeh, and R. Bakhtiari, "Preparation and optimization of ciprofloxacin encapsulated niosomes: A new approach for enhanced antibacterial activity, biofilm inhibition and reduced antibiotic resistance in ciprofloxacin-resistant methicillin-resistance staphylococcus aureus", *Bioinorg Chem*, 103, 104231 (2020).
 22. B. Maddiboyina, M. Hanumanaik, R.K. Nakkala, V. Jhawat, P. Rawat, A. Alam, A.I. Foudah, M.M. Alrobaian, R. Shukla, and S. Singh, "Formulation and evaluation of gastro-retentive floating bilayer tablet for the treatment of hypertension", *Heliyon*, 6(11), e05459 (2020).
 23. S. K Shukla, V. Nguyen, M. Goyal, and V. Gupta, "Cationically modified inhalable nintedanib niosomes: Enhancing therapeutic activity against non-small-cell lung cancer", *Nanomed*, 17(13), 935-958 (2022).
 24. M. Yasser, M. Teaima, M. El-Nabarawi, and R.A. El-Monem, "Cubosomal based oral tablet for controlled drug delivery of telmisartan: Formulation, In-vitro evaluation and in-vivo comparative pharmacokinetic study in rabbits", *Drug Dev Ind Pharm*, 45(6), 981-994 (2019).
 25. M.G.S. Correia, M.L. Briuglia, F. Niosi, and D.A. Lamprou, "Microfluidic manufacturing of phospholipid nanoparticles: Stability, encapsulation efficacy, and drug release", *Int J Pharm*, 516(1-2), 91-99 (2017).
 26. M.E. El-Haddad, A.A. Hussien, H.M. Saeed, and R.M. Farid, "Down regulation of inflammatory cytokines by the bioactive resveratrol-loaded chitoniosomes in induced ocular inflammation model", *J Drug Deliv Sci Technol*, 66, 102787 (2021).
 27. V. Gugleva, S. Titeva, N. Ermenlieva, S. Tsibranska, S. Tcholakova, S. Rangelov, and D. Momekova, "Development and evaluation of doxycycline niosomal thermoresponsive in situ gel for ophthalmic delivery", *Int J Pharm*, 591, 120010 (2020).
 28. N. Morsi, D. Ghorab, H. Refai, and H. Teba, "Ketorolac tromethamine loaded nanodispersion incorporated into thermosensitive in situ gel for prolonged ocular delivery", *Int J Pharm*, 506(1-2), 57-67 (2016).
 29. A.M. Fahmy, D.A. El-Setouhy, A.B. Ibrahim, B.A. Habib, S.A. Tayel, and N.A. Bayoumi, "Penetration enhancer-containing spanlastics (peccs) for transdermal delivery of haloperidol: In vitro characterization, ex vivo permeation and in vivo biodistribution studies", *Drug Deliv*, 25(1), 12-22 (2018).
 30. M. Dholakia, V. Thakkar, N. Patel, and T. Gandhi, "Development and characterisation of thermo reversible mucoadhesive moxifloxacin hydrochloride in situ ophthalmic gel", *J Pharm Bioallied Sci*, 4(5), 42 (2012).
 31. S. Mandal, M.K. Thimmasetty, G. Prabhushankar, and M. Geetha, "Formulation and evaluation of an in situ gel-forming ophthalmic formulation of moxifloxacin hydrochloride", *Int J Pharm Investig*, 2(2), 78 (2012).
 32. H. Shelley, R.M. Rodriguez-Galarza, S.H. Duran, E.M. Abarca, and R.J. Babu, "In situ gel formulation for enhanced ocular

- delivery of nepafenac", *J Pharm Sci*, 107(12), 3089-3097 (2018).
33. J. Lou, W. Hu, R. Tian, H. Zhang, Y. Jia, J. Zhang, and L. Zhang, "Optimization and evaluation of a thermoresponsive ophthalmic in situ gel containing curcumin-loaded albumin nanoparticles", *Int J Nanomedicine*, 9, 2517 (2014).
 34. R. Asasutjarit, S. Thanasanchokpibull, A. Fuongfuchat, and S. Veeranondha, "Optimization and evaluation of thermoresponsive diclofenac sodium ophthalmic in situ gels", *Int J Pharm*, 411(1-2), 128-135 (2011).
 35. P.D. Chaudhari and U.S. Desai, "Formulation and evaluation of niosomal in situ gel of prednisolone sodium phosphate for ocular drug delivery", *Int J Appl Pharm*, 97-116 (2019).
 36. D. Aggarwal, A. Garg, and I.P. Kaur, "Development of a topical niosomal preparation of acetazolamide: Preparation and evaluation", *J Pharm Pharmacol*, 56(12), 1509-1517 (2004).
 37. P. Shah, B. Goodyear, N. Dholaria, V. Puri, and B. Michniak-Kohn, "Nanostructured non-ionic surfactant carrier-based gel for topical delivery of desoximetasone", *Int J Mol Sci*, 22(4), 1535 (2021).
 38. M.K. Khan, B.A. Khan, B. Uzair, S.I. Niaz, H. Khan, K.M. Hosny, and F. Mena, "Development of chitosan-based nanoemulsion gel containing microbial secondary metabolite with effective antifungal activity: In vitro and in vivo characterizations", *Int J Nanomedicine*, 16, 8203-8219 (2021).
 39. M. Kouchak, M. Mahmoodzadeh, and F. Farrahi, "Designing of a pH-triggered carbopol®/hpmc in situ gel for ocular delivery of dorzolamide hcl: In vitro, in vivo, and ex vivo evaluation", *AAPS PharmSciTech*, 20(5), 1-8 (2019).
 40. K.M. Ranch, F.A. Maulvi, M.J. Naik, A.R. Koli, R.K. Parikh, and D.O. Shah, "Optimization of a novel in situ gel for sustained ocular drug delivery using box-behnken design: In vitro, ex vivo, in vivo and human studies", *Int J Pharm*, 554, 264-275 (2019).
 41. A. Manosroi, W. Ruksiriwanich, M. Abe, W. Manosroi, and J. Manosroi, "Transfollicular enhancement of gel containing cationic niosomes loaded with unsaturated fatty acids in rice (*oryza sativa*) bran semi-purified fraction", *Eur J Pharm Biopharm*, 81(2), 303-313 (2012).
 42. A. López-Machado, N. Díaz-Garrido, A. Cano, M. Espina, J. Badia, L. Baldomà, A.C. Calpena, E.B. Souto, M.L. García, and E. Sánchez-López, "Development of lactoferrin-loaded liposomes for the management of dry eye disease and ocular inflammation", *Pharmaceutics*, 13(10), 1698 (2021).
 43. B.S. Anand and A.K. Mitra, "Mechanism of corneal permeation of l-valyl ester of acyclovir: Targeting the oligopeptide transporter on the rabbit cornea", *Pharm Res*, 19(8), 1194-1202 (2002).
 44. S. Deepthi and J. Jose, "Novel hydrogel-based ocular drug delivery system for the treatment of conjunctivitis", *Int Ophthalmol*, 39(6), 1355-1366 (2019).
 45. J.E. Gebo and A.F. Lau, "Sterility testing for cellular therapies: What is the role of the clinical microbiology laboratory?", *J Clin Microbiol*, 58(7), e01492-01419 (2020).
 46. C. Dierks, R. Söldner, K. Prühl, N. Wagner, N. Delmdahl, A. Dominik, M.W. Olszowy, and J. Austerjost, "Towards an automated approach for smart sterility test examination", *SLAS Technol*, 27(6), 339-343 (2022).
 47. G.-H. Hsiue, R.-W. Chang, C.-H. Wang, and S.-H. Lee, "Development of in situ thermosensitive drug vehicles for glaucoma therapy", *Biomater*, 24(13), 2423-2430 (2003).
 48. K.R. Wilhelmus, "The draize eye test", *Surv Ophthalmol*, 45(6), 493-515 (2001).
 49. F. Lallemand, P. Furrer, O. Felt-Baeyens, M. Gex-Fabry, J.-M. Dumont, K. Besseghir, and R. Gurny, "A novel water-soluble cyclosporine a prodrug: Ocular tolerance and in vivo kinetics", *Int J Pharm*, 295(1-2), 7-14 (2005).
 50. J.W. Shell, "Ocular drug delivery systems - a review", *J toxicol Cutan ocul toxicol*, 1(1), 49-63 (1982).

51. H. Abdelkader, S. Ismail, A. Hussein, Z. Wu, R. Al-Kassas, and R.G. Alany, "Conjunctival and corneal tolerability assessment of ocular naltrexone niosomes and their ingredients on the hen's egg chorioallantoic membrane and excised bovine cornea models", *Int J Pharm*, 432(1-2), 1-10 (2012).
52. J. Bancroft, A. Stevens, and D. Turner, "Theory and practice of histological techniques, Churchill Livingstone", *New York, London, San Francisco, Tokyo* (1996).
53. M. Mokhtar, O.A. Sammour, M.A. Hammad, and N.A. Megrab, "Effect of some formulation parameters on flurbiprofen encapsulation and release rates of niosomes prepared from proniosomes", *Int J Pharm*, 361(1-2), 104-111 (2008).
54. T. Yoshioka, B. Sternberg, and A.T. Florence, "Preparation and properties of vesicles (niosomes) of sorbitan monoesters (span 20, 40, 60 and 80) and a sorbitan triester (span 85)", *Int J Pharm*, 105(1), 1-6 (1994).
55. M. Bashash, M. Varidi, and J. Varshosaz, "Sucrose stearate based niosomes as an alternative to ordinary vehicles for efficient curcumin delivery", *J Food Meas Charact*, 16(3), 2104-2118 (2022).
56. V. Akbari, D. Abedi, A. Pardakhty, and H. Sadeghi-Aliabadi, "Release studies on ciprofloxacin loaded non-ionic surfactant vesicles", *Avicenna J Med Biotechnol*, 7(2), 69 (2015).
57. B. Nasser, "Effect of cholesterol and temperature on the elastic properties of niosomal membranes", *Int J Pharm*, 300(1-2), 95-101 (2005).
58. S. Durak, M. Esmaili Rad, A. Alp Yetisgin, H. Eda Sutova, O. Kutlu, S. Cetinel, and A. Zarrabi, "Niosomal drug delivery systems for ocular disease—recent advances and future prospects", *Nanomater*, 10(6), 1191 (2020).
59. H. Abdelkader, U. Farghaly, and H. Moharram, "Effects of surfactant type and cholesterol level on niosomes physical properties and in vivo ocular performance using timolol maleate as a model drug", *J Pharm Investig*, 44(5), 329-337 (2014).
60. H. Alyami, K. Abdelaziz, E.Z. Dahmash, and A. Iyire, "Nonionic surfactant vesicles (niosomes) for ocular drug delivery: Development, evaluation and toxicological profiling", *J Drug Deliv Sci Technol*, 60, 102069 (2020).
61. D. Ag Seleci, M. Seleci, J.-G. Walter, F. Stahl, and T. Scheper, "Niosomes as nanoparticulate drug carriers: Fundamentals and recent applications", *J Nanomater*, 2016, 7372306 (2016).
62. T. Liu, R. Guo, W. Hua, and J. Qiu, "Structure behaviors of hemoglobin in peg 6000/tween 80/span 80/h₂o niosome system", *Colloids Surf A: Physicochem Eng Asp*, 293(1-3), 255-261 (2007).
63. G.N. Devaraj, S. Parakh, R. Devraj, S. Apte, B.R. Rao, and D. Rambhau, "Release studies on niosomes containing fatty alcohols as bilayer stabilizers instead of cholesterol", *J Colloid Interface Sci*, 251(2), 360-365 (2002).
64. A.S. Guinedi, N.D. Mortada, S. Mansour, and R.M. Hathout, "Preparation and evaluation of reverse-phase evaporation and multilamellar niosomes as ophthalmic carriers of acetazolamide", *Int J Pharm*, 306(1), 71-82 (2005).
65. D.S. Shaker, M.A. Shaker, and M.S. Hanafy, "Cellular uptake, cytotoxicity and in-vivo evaluation of tamoxifen citrate loaded niosomes", *Int J Pharm*, 493(1), 285-294 (2015).
66. T. Higuchi, "Rate of release of medicaments from ointment bases containing drugs in suspension", *J Pharm Sci*, 50(10), 874-875 (1961).
67. C.E. Mary Dacruz, P.J. Bhide, L. Kumar, and R.K. Shirodkar, "Novel nano spanlastic carrier system for buccal delivery of lacidipine", *J Drug Deliv Sci Technol*, 68, 103061 (2022).
68. A. Madni, M.A. Rahim, M.A. Mahmood, A. Jabar, M. Rehman, H. Shah, A. Khan, N. Tahir, and A. Shah, "Enhancement of dissolution and skin permeability of pentazocine by proniosomes and niosomal gel", *AAPS PharmSciTech*, 19(4), 1544-1553 (2018).
69. G.A. El-Emam, G.N. Girgis, M.M.A. El-Sokkary, O.A.E.-A. Soliman, and A.E.G.H. Abd El, "Ocular inserts of

- voriconazole-loaded proniosomal gels: Formulation, evaluation and microbiological studies", *Int J Nanomedicine*, 15, 7825 (2020).
70. L. Peltonen, "The interfacial behaviour of sorbitan surfactant monolayers and the bulk properties of these surfactants as a function of temperature", (2001).
 71. M.D. Milošević, M.M. Logar, A.V. Poharc-Logar, and N.L. Jakšić, "Orientation and optical polarized spectra (380-900 nm) of methylene blue crystals on a glass surface", *Int J Spectrosc*, 2013, 923739 (2013).
 72. A. Farmoudeh, J. Akbari, M. Saeedi, M. Ghasemi, N. Asemi, and A. Nokhodchi, "Methylene blue-loaded niosome: Preparation, physicochemical characterization, and in vivo wound healing assessment", *Adv Drug Deliv Rev*, 10(5), 1428-1441 (2020).
 73. Z. Sadeghi Ghadi and P. Ebrahimnejad, "Curcumin entrapped hyaluronan containing niosomes: Preparation, characterisation and in vitro/in vivo evaluation", *J Microencapsul*, 36(2), 169-179 (2019).
 74. B. Srividya, R.M. Cardoza, and P. Amin, "Sustained ophthalmic delivery of ofloxacin from a pH triggered in situ gelling system", *J Control Release*, 73(2-3), 205-211 (2001).
 75. A. El-Kamel, "In vitro and in vivo evaluation of pluronic f127-based ocular delivery system for timolol maleate", *Int J Pharm*, 241(1), 47-55 (2002).
 76. L. Klouda and A.G. Mikos, "Thermoresponsive hydrogels in biomedical applications", *Eur J Pharm Biopharm*, 68(1), 34-45 (2008).
 77. A.M. Bodratti and P. Alexandridis, "Formulation of poloxamers for drug delivery", *J Funct Biomater*, 9(1), 11 (2018).
 78. G. Dumortier, J.L. Grossiord, F. Agnely, and J.C. Chaumeil, "A review of poloxamer 407 pharmaceutical and pharmacological characteristics", *Pharm Res*, 23(12), 2709-2728 (2006).
 79. K. Al Khateb, E.K. Ozhmukhametova, M.N. Mussin, S.K. Seilkhanov, T.K. Rakhypbekov, W.M. Lau, and V.V. Khutoryanskiy, "In situ gelling systems based on pluronic f127/pluronic f68 formulations for ocular drug delivery", *Int J Pharm*, 502(1-2), 70-79 (2016).
 80. A. Fakhari, M. Corcoran, and A. Schwarz, "Thermogelling properties of purified poloxamer 407", *Heliyon*, 3(8), 390 (2017).
 81. H.Y. Kweon, J.H. Yeo, K.G. Lee, Y.W. Lee, Y.H. Park, J.H. Nahm, and C.S. Cho, "Effects of poloxamer on the gelation of silk sericin", *Macromol Rapid Commun*, 21(18), 1302-1305 (2000).
 82. E. Giuliano, D. Paolino, M. Fresta, and D. Cosco, "Mucosal applications of poloxamer 407-based hydrogels: An overview", *Pharmaceutics*, 10(3), 159 (2018).
 83. M. Gorcea and D. Laura, "Evaluating the physicochemical properties of emollient esters for cosmetic use", *Cosmet toiletries*, 125(12) (2010).
 84. M. Douguet, C. Picard, G. Savary, F. Merlaud, N. Loubat-bouleuc, and M. Grisel, "Spreading properties of cosmetic emollients: Use of synthetic skin surface to elucidate structural effect", *Colloids Surf B Biointerfaces*, 154, 307-314 (2017).
 85. G.D. Airey, "Rheological properties of styrene butadiene styrene polymer modified road bitumens", *Fuel*, 82(14), 1709-1719 (2003).
 86. G. Di Colo, Y. Zambito, S. Burgalassi, I. Nardini, and M.F. Saettone, "Effect of chitosan and of n-carboxymethylchitosan on intraocular penetration of topically applied ofloxacin", *Int J Pharm*, 273(1), 37-44 (2004).
 87. G.P. Andrews, S.P. Gorman, and D.S. Jones, "Rheological characterisation of primary and binary interactive bioadhesive gels composed of cellulose derivatives designed as ophthalmic viscosurgical devices", *Biomater*, 26(5), 571-580 (2005).
 88. L. Maggi, R. Bruni, and U. Conte, "High molecular weight polyethylene oxides (peos) as an alternative to hpmc in controlled release dosage forms", *Int J Pharm*, 195(1-2), 229-238 (2000).
 89. C. Maderuelo, A. Zarzuelo, and J.M. Lanao, "Critical factors in the release of

- drugs from sustained release hydrophilic matrices", *J Control Release*, 154(1), 2-19 (2011).
90. A. Verma, A. Tiwari, S. Saraf, P.K. Panda, A. Jain, and S.K. Jain, "Emerging potential of niosomes in ocular delivery", *Expert Opin Drug Deliv*, 18(1), 55-71 (2021).
 91. A. Salama, M. Badran, M. Elmowafy, and G.M. Soliman, "Spironolactone-loaded leciplexes as potential topical delivery systems for female acne: In vitro appraisal and ex vivo skin permeability studies", *Pharmaceutics*, 12(1), 25 (2020).
 92. T. Oka, T. Shearer, and M. Azuma, "Involvement of cyclooxygenase-2 in rat models of conjunctivitis", *Curr Eye Res*, 29(1), 27-34 (2004).
 93. M. Kato, Y. Hagiwara, T. Oda, M. Imamura-Takai, H. Aono, and M. Nakamura, "Beneficial pharmacological effects of selective glucocorticoid receptor agonist in external eye diseases", *J Ocul Pharmacol Ther*, 27(4), 353-360 (2011).
 94. R. Salmazi, G. Calixto, J. Bernegossi, M.A. dos Santos Ramos, T.M. Bauab, and M. Chorilli, "A curcumin-loaded liquid crystal precursor mucoadhesive system for the treatment of vaginal candidiasis", *Int J Nanomedicine*, 10, 4815 (2015).



نشرة العلوم الصيدلانية جامعة أسيوط



الهلام المحمل بالنيوزومات المحتوية على عقار السيليكوكسيب كنظام توصيل دوائى قيم لالتهاب العين

محمد سيد أحمد^١ - إكرامى عبد الرحيم خليل^{١*} - خالد حسانين محمد أحمد^٢ -
جمال الدين عبد الفتاح الجندى^١ - سيد إسماعيل محمد^١

^١ قسم الصيدلانيات، كلية الصيدلة، جامعة أسيوط، أسيوط، مصر

^٢ قسم الباثولوجى، كلية الطب البيطرى، جامعة أسيوط، أسيوط، مصر

النيوزومات هي ناقلات واعدة متناهية الصغر لتوصيل الأدوية للعين لأن لها القدرة على تعزيز التوافر الحيوي والفعالية للأدوية المختلفة. وفي الوقت نفسه، فإن المواد الهلامية الموضعية مفيدة لعلاج التهاب العين لأنها تحسن نفاذية القرنية وتزيد من وقت التلامس مع سطح العين، ويعتبر الغرض الرئيسي من هذه الدراسة هو إعداد وتقييم المواد الهلامية المحملة بالنيوزومات لتوصيل عقار السيليكوكسيب داخل العين، وقد تم تحضير نيوزومات مختلفة باستخدام مواد خافضة للتوتر السطحي مختلفة (السيبان ٦٠ والسيبان ٤٠) والكوليسترول (٣٠-٥٠ مول كنسبة مئوية)، وتتميز التركيبة المثالية المحضرة من السيبان ٤٠ والكوليسترول (نسبة ٣:٧) بكفاءة تغليف عالية نسبياً (~٥٧%) مع حجم جسيمات مناسبة للتوصيل للعين (~٣٤٨ نانومتر)، وقد أظهرت أعلى معدل إطلاق للدواء (~٦٥%) بعد ٢٤ ساعة مقارنة بالتحضيرات الأخرى، ثم تم استخدام التركيبة المثالية المحسنة لتحضير هلام محمل بالنيوزومات المحتوية على عقار السيليكوكسيب وكذلك تحضير الهيدروجيل الموضعي المحمل بالنيوزومات المحتوية على عقار السيليكوكسيب، كانت المواد الهلامية والهيدروجيل الموضعي جيدة التحمل من قبل العين وأظهرت تماثل بينهما في إختراق السيليكوكسيب للقرنية، ومع ذلك فقد أظهرت المواد الهلامية تأثيراً أعلى لعلاج التهابات القرنية مقارنة بالهيدروجيل الموضعي وقطرة العين ديكلوفيناك (ايبيفيناك) المتاحة تجارياً، تشير النتائج الموضحة في هذه الدراسة إلى أن الهلام المحمل بالنيوزومات المحتوية على عقار السيليكوكسيب هو نظام توصيل دواء قيم لالتهاب العين.